A Variational Learning Approach for Concurrent Distance Estimation and Environmental Identification

Yuxiao Li, *Student Member, IEEE,* Santiago Mazuelas, *Senior Member, IEEE,* and Yuan Shen, *Senior Member, IEEE*

***Abstract*—Wireless propagated signals encapsulate rich information for high-accuracy localization and environment sensing. However, the full exploitation of positional and environmental features as well as their correlation remains challenging in complex propagation environments. In this paper, we propose a methodology of variational inference over deep neural networks for concurrent distance estimation and environmental identification. The proposed approach, namely inter-instance variational auto-encoders (IIns-VAEs), conducts inference with latent variables that encapsulate information about both distance and environmental labels. A deep learning network with instance normalization is designed to approximate the inference concurrently via deep learning. We conduct extensive experiments on real-world datasets and the results show the superiority of the proposed IIns-VAE in both distance estimation and environmental identification compared to conventional approaches.**

***Index Terms*—Wireless signals, variational inference, deep learning, distance estimation, environmental identification.**

I. Introduction

WIRELESS propagated signals can offer rich information, such as positional and environmental features, related to the situation awareness of a user equipment [1]–[4]. Situational awareness is targeted to obtain accurate and reliable information for enhanced localization [5]–[8] and environment sensing [9]–[12]. Such techniques can enable a wide range of wireless applications, including autonomous driving [8], crowd sensing [13], environmental monitoring [14], and smart cities [15]. Hence, effective methods for high-accuracy localization and environmental sensing in complex propagation environments are increasingly important for wireless applications, promising to open a new paradigm for beyond fifth-generation (B5G) network requirements [16].

Manuscript received xx xx 2022; revised xx xx 2022; accepted xx xx 2023. Date of publication XXX; date of current version XXX. This work was supported in part by the Shanghai AI Laboratory, the National Natural Science Foundation of China under Grant 62271285, the Tsinghua University – OPPO Joint Research Institute, the Project PID2019-105058GA-I00 funded by MCIN/AEI/10.13039/501100011033, and the ELKARTEK programme funded by the Basque Government. The review of this article was coordinated by Prof. xx. *(Corresponding author: Yuan Shen.)*

Yuxiao Li is with the Department of Electronic Engineering and the Beijing National Research Center for Information Science and Technology, Tsinghua University, Beijing 100084, China. (e-mails: li-yx18@mails.tsinghua.edu.cn).

Santiago Mazuelas is with the Basque Center for Applied Mathematics (BCAM), 48009 Bilbao, Spain, and also with the IKERBASQUE Foundation for Science, 48009 Bilbao, Spain (e-mail: smazuelas@bcamath.org).

Yuan Shen is with the Department of Electronic Engineering and the Beijing National Research Center for Information Science and Technology, Tsinghua University, Beijing 100084, China, and also with the Shanghai AI Laboratory, Shanghai 201112, China (e-mail: shenyuan_ee@tsinghua.edu.cn).

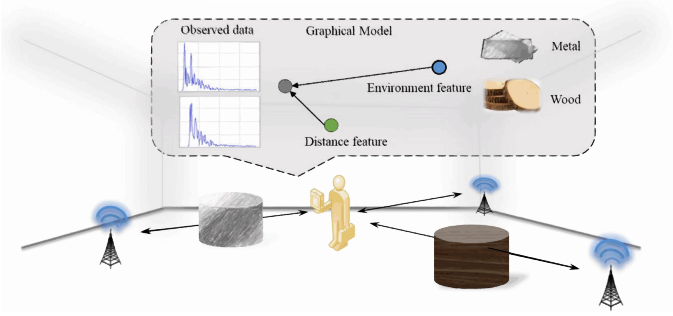

Fig. 1. Illustration of the proposed method. Distance and environmental features can be exploited from signals via variational inference on a graphical model. The latent variable for different environmental features can lead to different signal characteristics.

Localization algorithms are commonly based on range-related measurements, where the first estimated delay is adopted as the line-of-sight (LOS) path to perform distance estimation [17]. Though easy to implement, such method tend to introduce a positive bias in distance estimation caused by non-line-of-sight (NLOS) propagation [18], as well as a cluttering noise due to the multi-path effect [7], [19]. Multiple distance estimation techniques have been proposed to improve the estimation performance via the exploration of information in signal measurements. Conventional methods are mostly model-based, with a simplified model for signal propagation mechanism [20]–[22]. Such modeling leads to a transparent interpretation, but often does not fully extract the wireless signal information. Existing learning-based methods, based on Support Vector machine (SVM) [9], [23], and Gaussian process regression (GPR) [24], formulate estimation as a regression problem from physical features (PFs) of signals [25]. These features, however, may still lose information inherent in the high-dimensional signal measurements [25], [26].

The environmental identification problem is often conducted separately to distance estimation in existing works. Such techniques mostly utilize statistical features for coarse LOS and NLOS detection [9]. As in distance estimation, these features are either hand-crafted conducted by SVM [10], relevance vector machine (RVM) [11], or data-driven conducted by neural networks [12]. It has seldomly been addressed that more detailed identification tasks can also be conducted via propagated signals. For example, the detection of different

obstacles and geometric layouts of the room are essential for advanced wireless applications. Such advanced tasks can be enabled by the exploitation of high-level environmental semantics.

Recently, several deep learning (DL) methods have been proposed for location-related tasks. These methods take raw high-dimensional signal measurements as input and directly learn the mapping between these measurements and the corresponding distances [27]–[29]. Benefiting from a more thorough exploitation of signals, these methods show significant improvements compared to conventional methods [28], [29]. However, such methods assume an oversimplified one-to-one mapping between the distance and the measurements, neglecting other freedom in the signal propagation mechanism [30], [31]. Such deficiency in methodology tends to cause overfitting, where algorithms trained on data from one site could hardly generalize to a different site. Therefore, it is essential for DL-based methods to develop algorithms that can take environmental features into consideration and generalize well to different environmental settings.

In this paper, we propose a methodology of variational inference over deep neural networks for concurrent distance estimation and environmental identification, as depicted in Fig. 1. The methodology is further implemented by a novel variational auto-encoder (VAE). The inferred distance and environmental scenario can hence benefit further use in localization and environmental sensing. The main contributions of the paper are as follows.

- We propose a method for concurrent inference of distance and environmental scenario together with the corresponding latent variable model (LVM). The model accounts for both distance and environmental features in wireless signals and their inter-relations.
- We design a VI-driven DL algorithm, namely Inter-Instance VAE (IIns-VAE), for the concurrent distance estimation and environmental identification. Integrated with learning techniques, the algorithm can conduct inference on raw signals with effective generalization across different scenarios.
- We conduct extensive experiments that show the superiority of the proposed approach in both distance estimation and environmental identification compared to ML and DL approaches.

The remaining sections are organized as follows. Section II describes the problem of concurrent distance estimation and environmental identification. Section III formulates the problem as concurrent inference in a LVM. Section IV proposes the variational learning method for the inference and presents IIns-VAE, a DL network structure to conduct the inference. The performance of the approach is evaluated in Section VI. Finally, Section VII concludes the paper.

Notations: random variables (RVs) are displayed in sans serif, upright fonts and their realizations in serif, italic fonts; vectors are denoted by bold lowercase letters; a RV and its realization are denoted by x and x; a random vector and its realization are denoted by $\mathbf{x}$ and $\boldsymbol{x}$; $\boldsymbol{x}[j]$ denotes the jth component of the vector $\boldsymbol{x}$; $p(\boldsymbol{x}|y)$ denotes the conditional distribution of $\mathbf{x}$ given $\mathsf{y} = y$; $\mathcal{N}(\boldsymbol{x}; \boldsymbol{\mu}, \boldsymbol{\Sigma})$ denotes the PDF of a Gaussian RV $\mathbf{x}$ with mean $\boldsymbol{\mu}$ and covariance matrix $\boldsymbol{\Sigma}$; $\mathbb{E}\{\cdot\}$ denotes the expectation of the argument, and $\mathbb{E}_{\mathbf{x}}\{\cdot\}$ denotes the expectation with respect to RV $\mathbf{x}$; sets are denoted by calligraphic fonts, e.g., $\mathcal{D}$.

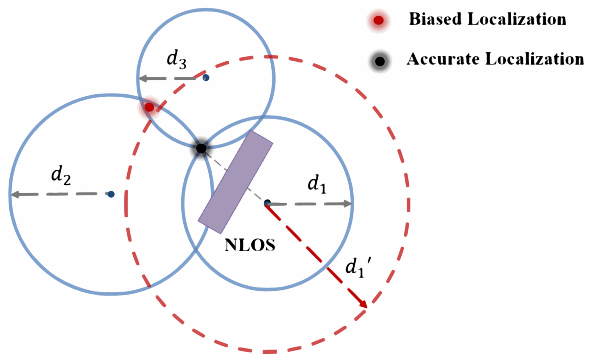

Fig. 2. Illustration of triangulation-based localization. The position of the target agent is inferred to be at the intersection of circles defined by the estimated distances. The NLOS condition can lead to a biased distance estimate that results in inaccurate localization.

II. Problem Statement

In this section, we introduce the distance estimation and environmental identification problem as well as the evaluation metrics.

A. Signal Model in Complex Environments

Complex propagation environments refer to wireless environments with NLOS conditions, multipath effects, and heavy scattering of signals [7], [32], such as indoor scenarios [33], [34]. A widely-adopted model of the received signal for range-based localization is as an aliased version of multiple replicas of transmitted signal plus additional noise, given by

$$\mathsf{x}(t) = \sum_{l=1}^{L} \alpha_l s(t - \tau_l) + \mathsf{n}(t), \ t \in [0, T_{\text{ob}}] \tag{1}$$

where $s(t)$ is the transmitted signal, L is the number of multipath components, α_l and τ_l are the amplitude and propagation delay of the lth component, respectively, $\mathsf{n}(t)$ is an additive white Gaussian noise (AWGN), and $[0, T_{\text{ob}}]$ is the observation interval. The signal after sampling can be represented as a random vector $\mathbf{x} \in \mathbb{R}^M$, where M denotes the length of the signal.

The relationship between the true distance d and delays of the propagation path is given by

$$\tau_l = \frac{1}{c}(d + b_l) \tag{2}$$

where c is the propagation speed of the signal, and $b_l > 0$ is the range bias of the $l-$th path. The associated signal component with $l = 1$ is called the first path (FP) component, while components with $l > 1$ are called multipath components (MPCs). The agent can compute its position from distance estimates by means of trilateration, via the intersection of circles determined by the estimated distances from anchors. The bias of distance estimation would deteriorate localization

performance and results in an inaccurate position estimation, as depicted in Fig. 2.

B. Concurrent Distance Estimation and Environmental Identification

We consider concurrent distance estimation and environmental identification problem, based on the received signal measurements. We denote the real distance between an anchor and an agent as d, and the label of environmental scenarios where the signal is measured as k, with $d \in [0, d_{\max}]$ and $k \in \mathcal{K} = \{0, 1, \ldots, K-1\}$. The meaning of the environmental scenario label set $\mathcal{K}$ can be different depending on the case. For example, in a roughly labeled case, the environmental label denotes LOS and NLOS conditions, i.e., $k \in \mathcal{K}_{\text{LOS}} = \{0, 1\}$ with $k = 0$ for LOS and $k = 1$ for NLOS conditions. The environmental label set can have more elaborated versions, including $\mathcal{K}_{\text{obs}}$ for different blocking obstacles, as well as $\mathcal{K}_{\text{room}}$ for different room geometric characteristics. In this paper, we develop techniques to concurrently estimate distance d and identify environmental scenario k given signal measurements $\boldsymbol{x}$. Moreover, we take both rough and elaborated label sets into consideration in experiments.

C. Evaluation Metrics

We introduce the evaluation metrics utilized for the estimation and identification problem. For distance estimation, we adopt two metrics for performance evaluation: the root mean square error (RMSE) and the mean absolute error (MAE). Specifically, the RMSE and MAE measured for N instances are defined as

$$\text{RMSE} = \sqrt{\frac{1}{N}\sum_{i=1}^{N}(\hat{d}^{(n)} - d^{(n)})^2} \tag{3}$$

$$\text{MAE} = \frac{1}{N}\sum_{i=1}^{N}\|\hat{d}^{(n)} - d^{(n)}\| \tag{4}$$

where n is the index of instances with real distance $d^{(n)}$ and estimated distance $\hat{d}^{(n)}$, $n = 1, 2, \ldots, N$.

For environmental identification, we utilize averaged identification accuracy for performance evaluation. Specifically, suppose the estimated label of the environmental scenario is $\hat{k}$ and the real environmental label is k, the accuracy for N instances is defined as

$$\text{ACC} = \frac{1}{N}\sum_{n=1}^{N}\mathbf{1}(\hat{k}^{(n)} = k^{(n)}) \tag{5}$$

where $k,\ k^* \in \{1, 2, ..., K\}$, $\mathbf{1}(k^{(n)} = k^{(n)*})$ is the indicator function and equal to one if the the nth prediction $k^{(n)}$ equals to the true environmental label k^*.

We further consider the execution time, the floating point operations (FLOPs), and the total parameter number to evaluate the computational efficiency and complexity of the DL network. These metrics provide insights for the potential employment in different real-world devices.

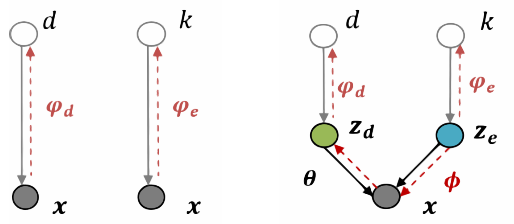

(a) (b)

Fig. 3. Graphical models for the inference of distance d and propagation environment k based on signal measurements $\boldsymbol{x}$. Solid lines denote the generative process and dashed lines denote the inference process. (a) The graphical model for conventional approaches, where inference problems are considered separately. (b) The graphical model for concurrent inference of distance d and propagation environment k.

III. Latent Variable Model for Concurrent Inference

In this section, we formulate the concurrent distance estimation and environmental identification as an inference problem on an LVM. We first introduce the model motivations driven by experimental observations and describe the LVM with latent variables for distance and environmental features. Then the VI method is introduced to conduct inference on an LVM. Note that though the method is formulated with distance-related signal measurements, it is applicable to signal measurements related to any positional metrics (such as angle, velocity, and acceleration).

A. Domain Knowledge of Environment

Complex propagation environments have a critical influence on signal measurements, and in turn on the distance estimate. We analyze their effects from the perspectives of both physical mechanisms and observations. We also conducted empirical analysis on real-world data in Section VI to further validate such impacts.

The NLOS condition is a most dominant environmental aspect for signal measurements in complex propagation environments. Generally, the NLOS condition can be detected from the signal distortion, including delay increase and reduced power in the first path (FP). More specific environmental features associated with NLOS condition can be analyzed in terms of the material of blocking obstacles. Since the propagated signals are electromagnetic waves, the reflection and transmission effects depend mainly on the electromagnetic properties of the obstacle materials. Specifically, the blocking materials in NLOS path can be classified into two categories: insulators and conductors. The insulators are relatively transparent to signals, resulting in less severe NLOS impact to signals. The conductors, on the other hand, will reflect most of the signal and cause significant excess delay and power reduction.

The multipath effect is another essential environmental aspect, especially in complex propagation environments like indoors. For example, rooms with larger size and sparser obstacles tend to have fewer MPCs from the walls. Distance

estimate in such cases can benefit from the usage of MPCs as side information.

NLOS condition and multipath effect directly impact the received signals, causing distortion in FP and MPCs. Therefore, such received signals can be used for the identification of different environmental scenarios. Specifically, the NLOS path in observed signals can be used for obstacle-level environmental identification. The signal measurements with MPCs can be used for room-level environmental identification. Several works have modeled mathematically the relationship between wireless propagated signals and different environmental scenarios [33], [35]–[37]. In particular, the additional position-related information yielded by geometrically modeled MPC is quantified in signal-to-interference-plus-noise ratio (SINR) values in [35].

Signal measurements contain both distance features and environmental features. The former can be used for distance estimation with accuracy influenced by the latter, whereas the latter can be used for the identification of different environmental scenarios. Motivated by these observations, we propose a methodology to conduct variational inference over deep neural networks for distance estimation and environmental identification. Such concurrent inference can be conducted jointly, and the usage of complementary information can improve inferences.

B. LVM for Concurrent Inference

Let x denote the RV for signal measurements. According to the analysis above, we define two latent variables for the generation of x. These variables are related to distance and environmental features inherent in x, denoted as positional variable z_d and environmental variable z_e, respectively. The LVM contains the signal measurements variable x, latent variables z_d, z_e, label variable d for distance, and label variable k for propagation environment.

Assumption 1. (Distance and Environmental Latent Variables) In the following we use the assumptions:

1) In the absence of measurements, the distance d and environmental scenario k are independent,
$$p(d,k) = p(d)p(k) \tag{6}$$
2) The latent variable $\boldsymbol{z}_\mathrm{d}$ is independent of k and $\boldsymbol{z}_\mathrm{e}$ given distance d, and the latent variable $\boldsymbol{z}_\mathrm{e}$ is independent of d and $\boldsymbol{z}_\mathrm{d}$ given environmental label k,
$$p(\boldsymbol{z}_\mathrm{d}, \boldsymbol{z}_\mathrm{e}|d,k) = p(\boldsymbol{z}_\mathrm{d}|d)p(\boldsymbol{z}_\mathrm{e}|k) \tag{7}$$
3) The signal measurement $\boldsymbol{x}$ is independent of d and k given $\boldsymbol{z}_\mathrm{d}$ and $\boldsymbol{z}_\mathrm{e}$,
$$p(\boldsymbol{x}|\boldsymbol{z}_\mathrm{d}, \boldsymbol{z}_\mathrm{e}, d, k) = p(\boldsymbol{x}|\boldsymbol{z}_\mathrm{d}, \boldsymbol{z}_\mathrm{e}) \tag{8}$$

Such assumptions describe the generative process of signal measurements $\boldsymbol{x}$ in the LVM, graphically shown as solid lines in Fig. 3b. The process implies the decomposition

$$p(\boldsymbol{x}, \boldsymbol{z}_\mathrm{d}, \boldsymbol{z}_\mathrm{e}, d, k) = p(d)p(k)p(\boldsymbol{z}_\mathrm{d}|d)p(\boldsymbol{z}_\mathrm{e}|k)p(\boldsymbol{x}|\boldsymbol{z}_\mathrm{d}, \boldsymbol{z}_\mathrm{e})\,. \tag{9}$$

Therefore, the inference for distance and environmental scenario can be conducted by the following sequential steps: i) Estimate latent variables $\boldsymbol{z}_\mathrm{d}$ and $\boldsymbol{z}_\mathrm{e}$ based on signal measurements $\boldsymbol{x}$; ii) Estimate the distance d based on distance features $\boldsymbol{z}_\mathrm{d}$; iii) Estimate the propagation environment k based on environmental features $\boldsymbol{z}_\mathrm{e}$.

C. Variational Inference Method

According to the LVM above, the inference for distance and propagated environment is conducted by first estimating latent variables $\boldsymbol{z}_\mathrm{d}$ and $\boldsymbol{z}_\mathrm{e}$, and then labels d and k from latent variables. Based on the VI method, we construct the variational distribution $q(\boldsymbol{z}_\mathrm{d}, \boldsymbol{z}_\mathrm{e}|\boldsymbol{x};\boldsymbol{\phi})$ to approximate the intractable posterior $p(\boldsymbol{z}_\mathrm{d}, \boldsymbol{z}_\mathrm{e}|\boldsymbol{x})$. Specifically, we take $q(\boldsymbol{z}_\mathrm{d}, \boldsymbol{z}_\mathrm{e}|\boldsymbol{x};\boldsymbol{\phi})$ from a parametric family satisfying (10) with its PDF differentiable almost everywhere with respect to $\boldsymbol{x}$ and $\boldsymbol{\phi}$.

In the offline step, we first estimate the distribution $p(\boldsymbol{z}_\mathrm{d}, \boldsymbol{z}_\mathrm{e}|\boldsymbol{x})$ given $\boldsymbol{x}$ as observed data. We then estimate distributions $p(d|\boldsymbol{z}_\mathrm{d})$ and $p(k|\boldsymbol{z}_\mathrm{e})$. In the online step afterwards, the estimation of latent variables $\boldsymbol{z}_\mathrm{d}$, $\boldsymbol{z}_\mathrm{e}$, and target variables d, k can be achieved by maximum a posterior (MAP) estimation given the distributions. In order to specify the VI method, we further make the following assumptions for algorithm derivation.

Assumption 2. (Parametric Variational Distributions) In the following we use the assumptions:

1) According to the mean-field assumption in VI [38], we assume that the variational distributions of the two latent variables are independent as follows
$$q(\boldsymbol{z}_\mathrm{d}, \boldsymbol{z}_\mathrm{e}|\boldsymbol{x};\boldsymbol{\phi}) = q(\boldsymbol{z}_\mathrm{d}|\boldsymbol{x};\boldsymbol{\phi}_\mathrm{d})q(\boldsymbol{z}_\mathrm{e}|\boldsymbol{x};\boldsymbol{\phi}_\mathrm{e}) \tag{10}$$
with $\boldsymbol{\phi} = \{\boldsymbol{\phi}_\mathrm{d}, \boldsymbol{\phi}_\mathrm{e}\}$ for convenience.
2) For network parameter learning, we assume that the conditional distribution on measurements variable $p(\boldsymbol{x}|\boldsymbol{z}_\mathrm{d}, \boldsymbol{z}_\mathrm{e};\boldsymbol{\theta})$ is from a parametric family of distributions with parameters $\boldsymbol{\theta}$. The conditional distributions on label variables $p(d|\boldsymbol{z}_\mathrm{d};\boldsymbol{\varphi}_\mathrm{d})$ and $p(k|\boldsymbol{z}_\mathrm{e};\boldsymbol{\varphi}_\mathrm{e})$ are from parametric families with $\boldsymbol{\varphi}_\mathrm{d}$ and $\boldsymbol{\varphi}_\mathrm{e}$. Likewise, their PDFs are assumed to be differentiable almost everywhere with respect to both conditioned variables and parameters.

The estimation of unknown distributions can be conducted by VI technique. The following proposition gives the evidence lower bound (ELBO) that enables such estimation.

Proposition 1: If *Assumptions 1-2* are satisfied, we have that for each instance-labels pair $(\boldsymbol{x}, d, k)$,

$$\begin{aligned}\mathcal{L}_\mathrm{ELBO}(\boldsymbol{x}, d, k;\boldsymbol{\phi},\boldsymbol{\theta},\boldsymbol{\varphi}) = {}& \mathbb{E}_{q(\boldsymbol{z}_\mathrm{d},\boldsymbol{z}_\mathrm{e}|\boldsymbol{x};\boldsymbol{\phi})}\big\{\log p(\boldsymbol{x}|\boldsymbol{z}_\mathrm{d}, \boldsymbol{z}_\mathrm{e};\boldsymbol{\theta})\big\} \\ & - \mathrm{D}_\mathrm{KL}\left(q(\boldsymbol{z}_\mathrm{d}, \boldsymbol{z}_\mathrm{e}|\boldsymbol{x};\boldsymbol{\phi})\big\|p(\boldsymbol{z}_\mathrm{d}, \boldsymbol{z}_\mathrm{e})\right) \\ & + \mathbb{E}_{q(\boldsymbol{z}_\mathrm{d}|\boldsymbol{x};\boldsymbol{\phi})}\big\{\log p(d|\boldsymbol{z}_\mathrm{d};\boldsymbol{\varphi})\big\} \\ & + \mathbb{E}_{q(\boldsymbol{z}_\mathrm{e}|\boldsymbol{x};\boldsymbol{\phi})}\big\{\log p(k|\boldsymbol{z}_\mathrm{e};\boldsymbol{\varphi})\big\} \\ \leq {}& \log\, p(\boldsymbol{x}, d, k)\,.\end{aligned} \tag{11}$$

In addition, the bound in (11) holds with equality if and only if $q(\boldsymbol{z}_\mathrm{d}, \boldsymbol{z}_\mathrm{e}|\boldsymbol{x}, d, k)$ matches the true posterior $p(\boldsymbol{z}_\mathrm{d}, \boldsymbol{z}_\mathrm{e}|\boldsymbol{x}, d, k)$ perfectly, i.e., $q(\boldsymbol{z}_\mathrm{d}, \boldsymbol{z}_\mathrm{e}|\boldsymbol{x}, d, k) = p(\boldsymbol{z}_\mathrm{d}, \boldsymbol{z}_\mathrm{e}|\boldsymbol{x}, d, k)$ for the instance-labels pair $(\boldsymbol{x}, d, k)$.

Proof: See Appendix A.

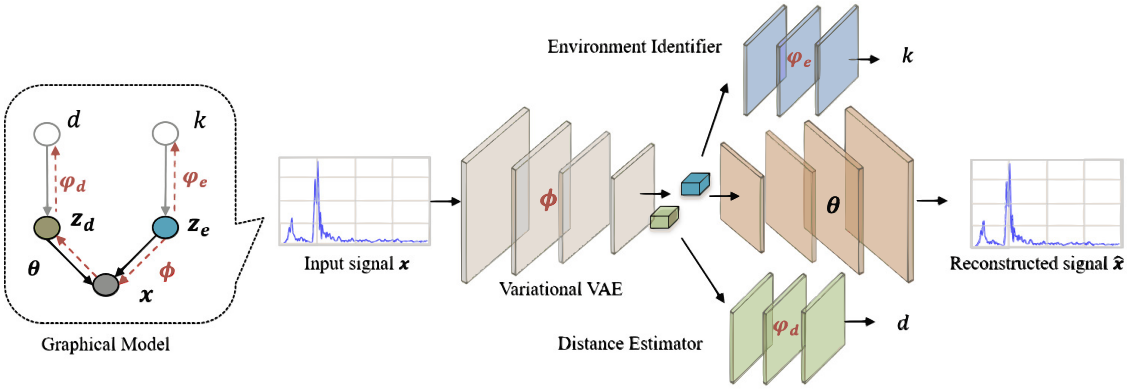

Fig. 4. Network structure of the proposed IIns-VAE for concurrent distance estimation and environmental identification. The received signal $\boldsymbol{x}$ is disentangled to distance feature $\boldsymbol{z}_{\rm d}$ and environment feature $\boldsymbol{z}_{\rm e}$ by the encoder, and reconstructed by the decoder. The estimator net utilizes $\boldsymbol{z}_{\rm d}$ for distance estimation, while the identifier net utilizes $\boldsymbol{z}_{\rm e}$ for environmental identification. The network parameters are trained on data under the guidance of the ELBO in the proposed LVM.

The ELBO described above is a lower bound on the log-likelihood of the observed data, with the gap being the KL divergence of the approximate from the true posterior. Therefore, maximum likelihood (ML) estimation can be approximated by maximizing the ELBO with respect to the unknown parameters. Suppose we are given a dataset $\mathcal{D} = \{\boldsymbol{x}^{(n)}, d^{(n)}, k^{(n)}\}_{n=1}^{N}$ with N i.i.d. data instances of signal measurements $\boldsymbol{x}$, real distance d, and environmental label k for parameters learning. The ELBO can be approximated by the sampling average on the instances in $\mathcal{D}$, denoted as $\mathcal{L}_{\text{ELBO},\mathcal{D}}$. Such empirical ELBO can then be used as the objective function to approximate ML estimation on the dataset $\mathcal{D}$ with respect to the intractable distributions. The estimation problem is then transformed to an optimization problem on distribution parameters, given as follow,

$$\boldsymbol{\phi}^*, \boldsymbol{\theta}^*, \boldsymbol{\varphi}^* = \arg\max_{\boldsymbol{\phi},\boldsymbol{\theta},\boldsymbol{\varphi}} \mathcal{L}_{\text{ELBO},\mathcal{D}}(\boldsymbol{x}, d, k; \boldsymbol{\phi}, \boldsymbol{\theta}, \boldsymbol{\varphi}). \tag{12}$$

Once the parameters $\boldsymbol{\phi}^*$, $\boldsymbol{\theta}^*$ and $\boldsymbol{\varphi}^*$ are obtained in the offline phase, the concurrent inference are conducted by the following steps:

1) Estimate distance and environmental features $\boldsymbol{z}_{\rm d}$ and $\boldsymbol{z}_{\rm e}$ from $\boldsymbol{x}$ based on $q(\boldsymbol{z}_{\rm d}, \boldsymbol{z}_{\rm e}|\boldsymbol{x}; \boldsymbol{\phi}^*)$.
2) Estimate distance d based on $p(d|\boldsymbol{z}_{\rm d}; \boldsymbol{\varphi}_{\rm d}^*)$ with distance feature $\boldsymbol{z}_{\rm d}$;
3) Estimate environmental scenario k based on $p(k|\boldsymbol{z}_{\rm e}; \boldsymbol{\varphi}_{\rm e}^*)$ with environmental feature $\boldsymbol{z}_{\rm e}$.

In the following, we describe the process to obtain optimal parameters $\boldsymbol{\phi}$, $\boldsymbol{\theta}$ and $\boldsymbol{\varphi}$ for the unknown distributions via deep learning.

IV. IIns-VAE Network Structure

This section proposes a DL network, namely the Inter-Instance VAE (IIns-VAE), to implement the concurrent inference of distance and environmental scenario based on raw signal measurements. We first transfer the objective function of VI to a parametric form, serving as the loss function for network training. Then a task-specific network structure is designed to conduct the inference, with instance normalization (IN) layers [39].

A. VAE-Based Network Structure

The VI method is targeted to estimate the variational posterior distribution $q(\boldsymbol{z}_{\rm d}, \boldsymbol{z}_{\rm e}|\boldsymbol{x}; \boldsymbol{\phi})$, as well as the intractable conditional distributions for likelihoods $p(\boldsymbol{x}|\boldsymbol{z}_{\rm d}, \boldsymbol{z}_{\rm e}; \boldsymbol{\theta})$, $p(d|\boldsymbol{z}_{\rm d}; \boldsymbol{\varphi}_{\rm d})$, and $p(k|\boldsymbol{z}_{\rm e}; \boldsymbol{\varphi}_{\rm e})$. We learn a deep generative network to approximate VI.

The network structure is presented in Fig. 4. The overall structure consists of four modules: a variational encoder with network parameters $\boldsymbol{\phi}$, a variational decoder with $\boldsymbol{\theta}$, a distance estimator network with $\boldsymbol{\varphi}_{\rm d}$, and an environment identifier network with $\boldsymbol{\varphi}_{\rm e}$. Note that the general framework proposed for variational learning can be utilized with general network structures. In particular, the approach proposed could also be implemented using other types of neural networks including residual network (ResNet) and long-short term memory (LSTM) networks.

In the offline training phase, the encoder takes in signal measurements $\boldsymbol{x}$ and disentangles features $\boldsymbol{z}_{\rm d}$ and $\boldsymbol{z}_{\rm e}$ via network parameters $\boldsymbol{\phi}$, i.e., $\boldsymbol{z}_{\rm d}, \boldsymbol{z}_{\rm e} \sim q(\boldsymbol{z}_{\rm d}, \boldsymbol{z}_{\rm e}|\boldsymbol{x}; \boldsymbol{\phi})$. The decoder samples features $\boldsymbol{z}_{\rm d}$ and $\boldsymbol{z}_{\rm e}$ as inputs and produces the reconstructed $\boldsymbol{x}$ via network parameters $\boldsymbol{\theta}$, i.e., $\hat{\boldsymbol{x}} \sim p(\boldsymbol{x}|\boldsymbol{z}_{\rm d}, \boldsymbol{z}_{\rm e}; \boldsymbol{\theta})$. The estimator net samples distance features $\boldsymbol{z}_{\rm d}$ and estimates d with parameters $\boldsymbol{\varphi}_{\rm d}$, i.e., $\hat{d} \sim p(d|\boldsymbol{z}_{\rm d}; \boldsymbol{\varphi}_{\rm d})$. The identifier, similarly, samples environment feature $\boldsymbol{z}_{\rm e}$ and produces estimates of propagation environment k via $\boldsymbol{\varphi}_{\rm e}$, i.e., $\hat{k} \sim p(k|\boldsymbol{z}_{\rm e}; \boldsymbol{\varphi}_{\rm e})$. The network learn these parameters with a loss derived from ELBO to guide training as described in the following.

B. Loss Function from Empirical ELBO

The following shows the specific loss function used to train a deep neural network shown in Fig. 4. Such loss function is obtained from the ELBO in (11) using the following approximations.

1) The prior over each latent variable is modeled by an isotropic multivariate Gaussian:

$$\begin{aligned} p(\boldsymbol{z}_{\rm d}) &= \mathcal{N}(\boldsymbol{z}_{\rm d}; \boldsymbol{0}, \epsilon_{\rm d}\boldsymbol{I}) \\ p(\boldsymbol{z}_{\rm e}) &= \mathcal{N}(\boldsymbol{z}_{\rm e}; \boldsymbol{0}, \epsilon_{\rm e}\boldsymbol{I}) \end{aligned} \tag{13}$$

where $\epsilon_{\rm d}$ and $\epsilon_{\rm e}$ are small values arbitrarily given to interpret randomness.

2) The distributioons of latent variables given received signals are modeled by Gaussian distributions, with means and variances learned by the encoder parameters $\boldsymbol{\phi}$:

$$\begin{aligned} q_{\boldsymbol{\phi}_{\rm d}}(\boldsymbol{z}_{\rm d}|\boldsymbol{x}) &= \mathcal{N}(\boldsymbol{z}_{\rm d}; \hat{\boldsymbol{\mu}}_{\rm d}, \hat{\boldsymbol{\sigma}}_{\rm d}^2 \boldsymbol{I}) \\ q_{\boldsymbol{\phi}_{\rm d}}(\boldsymbol{z}_{\rm e}|\boldsymbol{x}) &= \mathcal{N}(\boldsymbol{z}_{\rm e}; \hat{\boldsymbol{\mu}}_{\rm e}, \hat{\boldsymbol{\sigma}}_{\rm e}^2 \boldsymbol{I}) \end{aligned} \tag{14}$$

where $\boldsymbol{\phi} = \{\boldsymbol{\phi}_{\rm d}, \boldsymbol{\phi}_{\rm d}\}$, $\hat{\boldsymbol{\mu}}_{\rm d} = \hat{\boldsymbol{\mu}}(\boldsymbol{x}; \boldsymbol{\phi}_{\rm d}), \hat{\boldsymbol{\sigma}}_{\rm d}^2 = \hat{\boldsymbol{\sigma}}^2(\boldsymbol{x}; \boldsymbol{\phi}_{\rm d})$ denote prediction functions for distribution parameters of distance feature $\boldsymbol{z}_{\rm d}$ learned by the encoder, similar for $\hat{\boldsymbol{\mu}}_{\rm e}$ and $\hat{\boldsymbol{\sigma}}_{\rm e}^2$ of environment feature $\boldsymbol{z}_{\rm e}$.

We then derive the loss function for network training. We first define the encoder loss term, denoted as $\mathbb{L}_{\rm enc}(\boldsymbol{x}; \boldsymbol{\phi})$, introduced by the second KL divergence term in ELBO in (11). Given the assumptions in (10) and models in (13)-(14), the encoder loss can be calculated analytically from the KL term in (11), presented as follows:

$$\begin{aligned} \mathbb{L}_{\rm enc}(\boldsymbol{x}; \boldsymbol{\phi}) = \mathbb{E}_{p_{\mathcal{D}}(\boldsymbol{x})} \, {\rm D}_{\rm KL} \left(\mathcal{N}(\hat{\boldsymbol{\mu}}_{\rm d}, \hat{\boldsymbol{\sigma}}_{\rm d}^2 \boldsymbol{I}) \big| \big| \mathcal{N}(\boldsymbol{0}, \epsilon_{\rm d} \boldsymbol{I}) \right) \\ + \mathbb{E}_{p_{\mathcal{D}}(\boldsymbol{x})} \, {\rm D}_{\rm KL} \left(\mathcal{N}(\hat{\boldsymbol{\mu}}_{\rm e}, \hat{\boldsymbol{\sigma}}_{\rm e}^2 \boldsymbol{I}) \big| \big| \mathcal{N}(\boldsymbol{0}, \epsilon_{\rm e} \boldsymbol{I}) \right) \end{aligned} \tag{15}$$

We then define the decoder loss term, denoted as $\mathbb{L}_{\rm dec}(\boldsymbol{x}; \boldsymbol{\phi}, \boldsymbol{\theta})$, introduced by the first expectation term in (11). This can be approximated by the mean square error (MSE) between signal instance $\boldsymbol{x}$ from $\mathcal{D}$ and the corresponding $\hat{\boldsymbol{x}}$ reconstructed by the VAE, given as follows:

$$\mathbb{L}_{\rm dec}(\boldsymbol{x}; \boldsymbol{\phi}, \boldsymbol{\theta}) = \mathbb{E}_{p_{\mathcal{D}}(\boldsymbol{x})} \| \boldsymbol{x} - \hat{\boldsymbol{x}}(\boldsymbol{x}; \boldsymbol{\phi}, \boldsymbol{\theta}) \|^2 \tag{16}$$

where $\hat{\boldsymbol{x}}(\boldsymbol{x}; \boldsymbol{\phi}, \boldsymbol{\theta})$ denotes the signal instance reconstructed by the VAE based on $\boldsymbol{x}$ with parameters $\boldsymbol{\phi}$ and $\boldsymbol{\theta}$.

The last two expectations terms in the ELBO contribute to loss terms for the estimator and identifier networks. In particular, the estimator loss term $\mathcal{L}_{\rm reg}(\boldsymbol{x}, d; \boldsymbol{\phi}, \boldsymbol{\varphi}_{\rm d})$ derived from the second expectation can be achieved by the MSE loss. The identifier loss term $\mathcal{L}_{\rm cls}(\boldsymbol{x}, k; \boldsymbol{\phi}, \boldsymbol{\varphi}_{\rm e})$ derived from the third expectation term can be achieved by the cross-entropy (CE) loss. These loss terms are given as follows

$$\mathbb{L}_{\rm reg}(\boldsymbol{x}, d; \boldsymbol{\phi}, \boldsymbol{\varphi}_{\rm d}) = \mathbb{E}_{p_{\mathcal{D}}(\boldsymbol{x}, d)} \left\| d - \hat{d}(\boldsymbol{x}; \boldsymbol{\phi}, \boldsymbol{\varphi}_{\rm d}) \right\|^2 \tag{17}$$

$$\mathbb{L}_{\rm cls}(\boldsymbol{x}, k; \boldsymbol{\phi}, \boldsymbol{\varphi}_{\rm e}) = -\mathbb{E}_{p_{\mathcal{D}}(\boldsymbol{x}, k)} \log q(y_{\rm e}|\boldsymbol{x}; \boldsymbol{\phi}, \boldsymbol{\varphi}_{\rm e}) \tag{18}$$

where $\hat{d}(\boldsymbol{x}; \boldsymbol{\phi}, \boldsymbol{\varphi}_{\rm d})$ denotes the distance estimated by the encoder and the estimator network with parameters $\boldsymbol{\phi}$ and $\boldsymbol{\varphi}_{\rm e}$. Note that the reparameterization trick [40] is utilized in sampling features of latent variables $\boldsymbol{z}_{\rm d}$ or $\boldsymbol{z}_{\rm e}$ for $\mathbb{L}_{\rm dec}(\boldsymbol{x}; \boldsymbol{\phi}, \boldsymbol{\theta})$, $\mathbb{L}_{\rm reg}(\boldsymbol{x}, d; \boldsymbol{\phi}, \boldsymbol{\varphi}_{\rm d})$, and $\mathbb{L}_{\rm cls}(\boldsymbol{x}, k; \boldsymbol{\phi}, \boldsymbol{\varphi}_{\rm e})$. If $\boldsymbol{\epsilon}^{(l)} \sim \mathcal{N}(\boldsymbol{0}, \boldsymbol{I})$, $\boldsymbol{z}_{\rm d}^{(l)}, \mathbf{z}_{\rm e}^{(l)}$ are constructed by the learned mean and variance terms combined with sampling the additional distribution to form the estimation, i.e., $\boldsymbol{z}_{\rm d}^{(l)} = \hat{\boldsymbol{\mu}}_{\rm d} + \hat{\boldsymbol{\sigma}}_{\rm d}^2 \odot \boldsymbol{\epsilon}^{(l)}$, $\boldsymbol{z}_{\rm e}^{(l)} = \hat{\boldsymbol{\mu}}_{\rm e} + \hat{\boldsymbol{\sigma}}_{\rm e}^2 \odot \boldsymbol{\epsilon}^{(l)}$, where $\odot$ denotes the element-wise product. In this case, we can compute and differentiate the KL divergence without estimation, as suggested in [40].

Therefore, the total loss function on dataset $\mathcal{D}$ with network parameters $\boldsymbol{\phi}$, $\boldsymbol{\theta}$ and $\boldsymbol{\varphi}$ is the combination of the above loss terms as follows,

$$\begin{aligned} \mathbb{L}(\mathcal{D}; \boldsymbol{\phi}, \boldsymbol{\theta}, \boldsymbol{\varphi}) = \sum_{n=1}^{N} \mathbb{L}_{\rm enc}(\boldsymbol{x}^{(n)}; \boldsymbol{\phi}) + \mathbb{L}_{\rm dec}(\boldsymbol{x}^{(n)}; \boldsymbol{\phi}, \boldsymbol{\theta}) \\ + \mathbb{L}_{\rm reg}(\boldsymbol{x}^{(n)}, d^{(n)}; \boldsymbol{\phi}, \boldsymbol{\varphi}_{\rm d}) + \mathbb{L}_{\rm cls}(\boldsymbol{x}^{(n)}, k^{(n)}; \boldsymbol{\phi}, \boldsymbol{\varphi}_{\rm e}) \end{aligned} \tag{19}$$

Hence, the inference on LVM is conducted by addressing the optimization problem $\min_{\boldsymbol{\phi}, \boldsymbol{\theta}, \boldsymbol{\varphi}} \mathbb{L}(\mathcal{D}; \boldsymbol{\phi}, \boldsymbol{\theta}, \boldsymbol{\varphi})$ by means of stochastic gradient descent algorithm.

C. Instance Normalization for Disentanglement

The VI approximation presented above is versatile and allows to be plugged in general neural networks, with the basic structure in Fig. 5. In the following, we describe the proposed IIns-VAE network structure with IN [39] and adaptive instance normalization (AdaIN) [41] technique for the VAE module. The problem-specific network architecture can hence avoid the need for expensive network fine-tuning. These techniques integrate model knowledge implicitly, making the network learning more structured and informed.

We find that adding IN layers to the positional sub-encoder can remove the environmental feature while preserving the distance feature. Similar ideas have been verified to be effective for style transfer in computer vision [41] and voice conversion [42].

We first utilize IN in the encoder to normalize the distance feature. Let M denote the feature map of the output of the former convolutional layer, which is a $W-$dimensional array. To apply IN, we have to compute the mean μ_c and standard variation σ_c of the $c-$th channel feature map M_c.

$$\begin{aligned} \mu_c &= \frac{1}{W} \sum_{w=1}^{W} M_c[w] \\ \sigma_c &= \sqrt{\frac{1}{W} \sum_{w=1}^{W} (M_c[w] - \mu_c)^2 + \epsilon} \end{aligned} \tag{20}$$

where $M_c[w]$ is the $w-$th element in M_c, ϵ is a small value to avoid numerical instability. To achieve IN, each element in the array M_c is normalized into M_c' as follows:

$$M_c'[w] = \frac{M_c[w] - \mu_c}{\sigma_c} \tag{21}$$

where the normalized M_c' substitutes M_c as transformed features, and are processed by the following deep network layers. In this way, the domain information for environments is removed from the distance feature. In order to ensure the signal reconstruction without information loss, the encoder extracts such domain information in the environment feature.

We then use AdaIN in the variational decoder to combine these two features. In AdaIN layers, the decoder first normalizes the global information by IN, and the environmental encoder provides the global information. The formula is given as follows,

$$M_c'[w] = \gamma_c \frac{M_c[w] - \mu_c}{\sigma_c} + \beta_c \tag{22}$$

where μ_c and σ_c are computed as (20), γ_c and β_c for each channel are the linear transformation of the output of

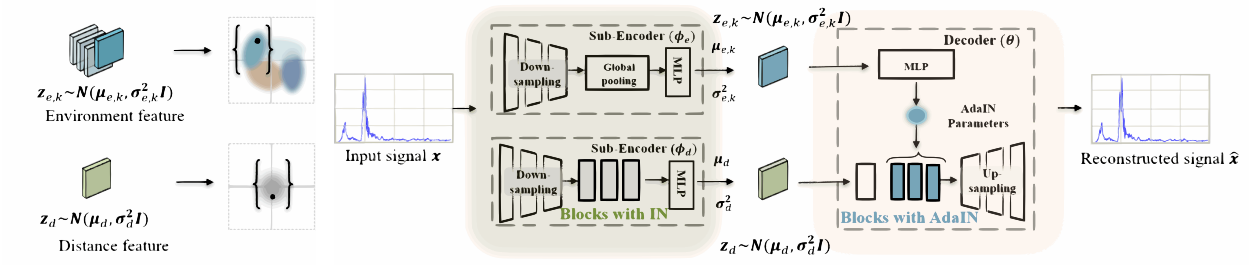

Fig. 5. Architecture of the VAE module in IIns-VAE. (a) Distributions of environment and distance features. (b) Architecture of the VAE module with IN [39] AdaIN [41] layers. The sub-encoder for distance feature contains IN [39] layers to extract instance-specific information and remove unspecific information. The decoder contains associated AdaIN [41] layers to combine both features and reconstruct the signal.

environment feature $\mathbf{z}_\mathrm{e}$. With these techniques, the combined feature integrates both instance-specific positional information as well as the instance-unspecific environmental information with respect to different environments, shown in Fig. 5b.

D. Deep Learning Algorithm

Given a dataset $\mathcal{D} = \{\boldsymbol{x}^{(n)}, d^{(n)}, k^{(n)}\}_{n=1}^{N}$ consisting of N i.i.d. instances with paired signal $\boldsymbol{x}$, real distance d, and environmental scenario k. The network approximate VI with dataset $\mathcal{D}$ by learning the distribution parameters $\boldsymbol{\phi}, \boldsymbol{\theta}, \boldsymbol{\varphi}_\mathrm{d}$ and $\boldsymbol{\varphi}_\mathrm{e}$. After these parameters are learned, the network can conduct concurrent inference of distance and propagation environment based on any received signals. Besides, the network automatically extract distance and environmental features as latent variables from signals as a side effect.

The offline training phase for parameters learning consists of four parallel parts:

1) The variational encoder with parameters $\boldsymbol{\phi}$ is learned on signal instance $\boldsymbol{x}^{(n)} \sim \mathcal{D}$ to produce two features $\boldsymbol{z}_\mathrm{d}^{(n)}$ and $\boldsymbol{z}_\mathrm{e}^{(n)}$, approximating the variational distribution $q(\boldsymbol{z}_\mathrm{d}, \boldsymbol{z}_\mathrm{e}|\boldsymbol{x}^{(n)}; \boldsymbol{\phi})$.
2) The variational decoder with $\boldsymbol{\theta}$ is learned on features $\boldsymbol{z}_\mathrm{d}^{(n)}$ and $\boldsymbol{z}_\mathrm{e}^{(n)}$ to produce the reconstructed signal instance $\boldsymbol{x}^{(n)}$, approximating the likelihood distribution $p(\boldsymbol{x}|\boldsymbol{z}_\mathrm{d}^{(n)}, \boldsymbol{z}_\mathrm{e}^{(n)}; \boldsymbol{\theta})$.
3) The estimator network with parameters $\boldsymbol{\varphi}_\mathrm{d}$ is learned on features $\boldsymbol{z}_\mathrm{d}^{(n)}$ to produce distance estimate $\hat{d}^{(n)}$, approximating the distribution $p(d|\boldsymbol{z}_\mathrm{d}^{(n)}; \boldsymbol{\varphi}_\mathrm{d})$.
4) The identifier network with parameters $\boldsymbol{\varphi}_\mathrm{e}$ is learned on features $\boldsymbol{z}_\mathrm{e}^{(n)}$ to produce environmental label estimate $\hat{k}^{(n)}$, approximating the likelihood distribution $p(k|\boldsymbol{z}_\mathrm{e}^{(n)}; \boldsymbol{\varphi}_\mathrm{e})$.

In the online testing phase, network parameters are frozen. The feature extraction and concurrent inference are conducted with the following three steps:

1) Feed signal instance $\boldsymbol{x}$ to encoder $\boldsymbol{\phi}^*$ for distance feature $\boldsymbol{z}_\mathrm{d}$ and environment feature $\boldsymbol{z}_\mathrm{e}$;
2) Feed distance feature $\boldsymbol{z}_\mathrm{d}$ into estimator $\boldsymbol{\varphi}_\mathrm{d}^*$ for the estimated distance $\hat{d}$;
3) Feed environment feature $\boldsymbol{z}_\mathrm{e}$ into identifier $\boldsymbol{\varphi}_\mathrm{e}^*$ for the estimated environmental scenario $\hat{k}$.

Since the network is learned in a unified scheme, distance estimation and environmental identification can be conducted concurrently. Algorithm 1 outlines the online and offline phases for training and utilizing IIns-VAE for the concurrent tasks.

While capable of concurrent inference, the trained IIns-VAE can conduct each downstream task separately according to the practical demand. For example, one can only conduct the first step for tasks where only the features are required, or the first two steps for distance estimation. Further downstream tasks potential to be enabled by IIns-VAE are discussed in Sec. V-B.

V. Discussion

The proposed IIns-VAE network has the following properties: i) It is driven by VI on the LVM specifically designed for wireless propagated signals; ii) It gives a novel network structure to approximate VI with deep learning; iii) It enables concurrent inference of distance and propagation environment based on high-dimensional signal measurements, as well as automatic extraction of distance and environmental features. The presented LVM and IIns-VAE algorithm can also introduce insights and variants on related problems. We briefly discuss some of the possible variants in this section.

A. Generalization to Semi-Supervised Learning

While formulated under the supervised learning scheme, the proposed approach can also be conducted in a border scenario for semi-supervised learning [43], [44]. Such scenario considers a dataset $\widetilde{\mathcal{D}}$ composed by an incomplete labeling of d and k. The acquisition of fully and accurately labeled data, especially for wireless scenarios, is often infeasible and at great cost of time, man-hour and money. In contrast, unlabeled data are much easier to obtain while also convey helpful modeling information [45]. Therefore, it is essential for DL-based approaches to tackle the scarcity of labeled data and evolve to the semi-supervised learning versions [45], [46].

In a semi-supervised learning scheme, the loss function can be assigned into a supervised term and an unsupervised term. In particular, the loss terms for the encoder, i.e., $\mathbb{L}_\mathrm{enc}(\boldsymbol{x}; \boldsymbol{\phi})$ and $\mathbb{L}_\mathrm{dec}(\boldsymbol{x}; \boldsymbol{\phi}, \boldsymbol{\theta})$ in (15)-(16), are fully unsupervised, based on signal measurements only. The loss terms for the estimator and the identifier, i.e., $\mathcal{L}_\mathrm{reg}(\boldsymbol{x}, d; \boldsymbol{\phi}, \boldsymbol{\varphi}_\mathrm{d})$ and $\mathcal{L}_\mathrm{cls}(\boldsymbol{x}, k; \boldsymbol{\phi}, \boldsymbol{\varphi}_\mathrm{e})$

Algorithm 1 Variational Learning of IIns-VAE

Offline Phase

Input: Training dataset $\mathcal{D} = \{\boldsymbol{x}^{(n)}, d^{(n)}, k\}_{n=1}^{N}$, learning rate α, batch size m, initial network parameters $\boldsymbol{\phi}_0$, $\boldsymbol{\theta}_0$, $\boldsymbol{\varphi}_{\mathrm{d},0}$ and $\boldsymbol{\varphi}_{\mathrm{e},0}$.

Output: Optimized parameters $\boldsymbol{\theta}^*, \boldsymbol{\phi}^*$, $\boldsymbol{\varphi}_{\mathrm{d}}^*$ and $\boldsymbol{\varphi}_{\mathrm{e}}^*$.

while $\boldsymbol{\phi}, \boldsymbol{\theta}, \boldsymbol{\varphi}_{\mathrm{d}}, \boldsymbol{\varphi}_{\mathrm{e}}$ have not converged **do**
  Sample a batch $\mathcal{B} = \{\boldsymbol{x}^{(n)}, d^{(n)}, k^{(n)}\}_{n=1}^{m} \sim \mathcal{D}$.
  $g_{\boldsymbol{\phi}}, g_{\boldsymbol{\theta}}, f_{\boldsymbol{\varphi}_{\mathrm{d}}}, f_{\boldsymbol{\varphi}_{\mathrm{e}}} \leftarrow \nabla \mathbb{L}(\mathcal{B}; \boldsymbol{\phi}, \boldsymbol{\theta}, \boldsymbol{\varphi}_{\mathrm{d}}, \boldsymbol{\varphi}_{\mathrm{e}})$.
  $\boldsymbol{\phi} \leftarrow \boldsymbol{\phi} + \alpha\, \mathrm{Adam}(\boldsymbol{\phi}, g_{\boldsymbol{\phi}})$.
  $\boldsymbol{\theta} \leftarrow \boldsymbol{\theta} + \alpha\, \mathrm{Adam}(\boldsymbol{\theta}, g_{\boldsymbol{\theta}})$.
  $\boldsymbol{\varphi}_{\mathrm{d}} \leftarrow \boldsymbol{\varphi}_{\mathrm{d}} + \alpha\, \mathrm{Adam}(\boldsymbol{\varphi}_{\mathrm{d}}, f_{\boldsymbol{\varphi}_{\mathrm{d}}})$.
  $\boldsymbol{\varphi}_{\mathrm{e}} \leftarrow \boldsymbol{\varphi}_{\mathrm{e}} + \alpha\, \mathrm{Adam}(\boldsymbol{\varphi}_{\mathrm{e}}, f_{\boldsymbol{\varphi}_{\mathrm{e}}})$.
end while

Online Phase

Input: New signal measurements $\boldsymbol{x}^{(n)}$, the stored model with parameters $\boldsymbol{\theta}^*, \boldsymbol{\phi}^*$, $\boldsymbol{\varphi}_{\mathrm{d}}^*, \boldsymbol{\varphi}_{\mathrm{e}}^*$.

Output: Estimated distance $\hat{d}^{(n)}$, environmental scenario $\hat{k}^{(n)}$.

for $n \geq 0$ **do**
  Generate $\boldsymbol{z}_{\mathrm{d}}^{(n)}$, $\boldsymbol{z}_{\mathrm{e}}^{(n)}$ from $\boldsymbol{x}^{(n)}$ via encoder parameters $\boldsymbol{\phi}^*$.

$$\boldsymbol{z}_{\mathrm{d}}^{(n)} \sim \mathcal{N}\big(\boldsymbol{z}_{\mathrm{d}}; \boldsymbol{\mu}(\boldsymbol{x}^{(n)}; \boldsymbol{\phi}^*); \boldsymbol{\sigma}^2(\boldsymbol{x}^{(n)}; \boldsymbol{\phi}^*)\mathbf{I}\big)$$
$$\boldsymbol{z}_{\mathrm{e}}^{(n)} \sim \mathcal{N}\big(\boldsymbol{z}_{\mathrm{e}}; \boldsymbol{\mu}(\boldsymbol{x}^{(n)}; \boldsymbol{\phi}^*); \boldsymbol{\sigma}^2(\boldsymbol{x}^{(n)}; \boldsymbol{\phi}^*)\mathbf{I}\big)$$

  Estimate $d^{(n)}$ from the distribution mean of ${\boldsymbol{z}_{\mathrm{d}}}^{(n)}$ via estimator parameters $\boldsymbol{\varphi}_{\mathrm{d}}^*$.

$$\hat{d}^{(n)} := \boldsymbol{\mu}(\boldsymbol{x}^{(n)}; \boldsymbol{\varphi}_{\mathrm{d}}^*)$$

  Estimate $k^{(n)}$ from the distribution mean of ${\boldsymbol{z}_{\mathrm{e}}}^{(n)}$ via the identifier parameters $\boldsymbol{\varphi}_{\mathrm{e}}^*$.

$$\hat{\boldsymbol{k}}^{(n)} := \boldsymbol{\mu}(\boldsymbol{x}^{(n)}; \boldsymbol{\varphi}_{\mathrm{e}}^*)$$

end for

in (17)-(18), are supervised based on signal-label pairs. We can assign a semi-supervised dataset to a supervised subset and an unsupervised subset, and use them to train the supervised and unsupervised loss terms respectively.

B. Variants in Downstream Tasks

In the proposed algorithms, the variational decoder and its learned parameters $\boldsymbol{\theta}$ are not used in the online phase. For the current estimation problem, they offer the regularization constraint to guide feature learning. However, the decoder and its approximated distribution $p(\boldsymbol{x}|\boldsymbol{z}_{\mathrm{d}}, \boldsymbol{z}_{\mathrm{e}})$ can be utilized as well. The decoder can work as a signal generator, enabling further downstream tasks like realistic signal simulation and conversion.

Signal simulation refers to the task of generating realistic propagated signals with the desired positional and environmental information. Similarly, signal conversion refers to the task where an input signal with targeted positional measurement but from a different propagated environment is converted to a target environment. With the proposed approach, these tasks can be achieved by combining the corresponding features in the decoder. The simulated signals can be used for indoor localization, channel condition estimation and other types of tasks, especially for learning-based methods in data-limited scenarios. Moreover, they can be applied to special information security tasks such as signal disguise.

C. Combination of Statistical Inference and Deep Learning

The proposed approach also presents a promising direction to bridge the gap between statistical inference and learning techniques. Such combination enjoys the benefits from both sides. On one hand, the proposed approach has the efficiency and capacity of DL techniques to approximate highly nonlinear transformations via training data. This addresses the cases with complicated and intractable distributions but accessible large datasets. Conventional statistical techniques for such cases tend to suffer from simplified assumptions to tackle intractability, and slow sampling process to process large dataset. On the other hand, the proposed approach enjoys the flexibility and transparent interpretation from statistic techniques. Motivated from first principles, the approach can avoid the overfitting problems in DL techniques. Moreover, the problem-oriented LVM enables more structured inference than conventional DL approaches. Therefore, the related methodology has the potential to enable a wide range of emerging applications, which can be both structured with LVM and complicated with intractable distributions.

VI. Experiments

In this section, we evaluate the proposed algorithms on datasets generated from two public UWB data campaigns. In particular, we give quantitative comparisons of the proposed approach and conventional techniques for distance estimation and environmental identification. Qualitative results of latent space visualization are also presented to illustrate the effectiveness of feature learning. In this section, we utilize UWB measurements but the proposed approach is technology-agnostic and applicable to any technology providing wireless propagated signals.

A. Public Databases

We utilize data from two publicly available databases on UWB. The data samples from these campaigns include received signal measurements, real distance labels, and environmental labels. We then generate three different datasets from them to test the proposed approach.

Database 1: The database is from [47], created using SNPN-UWB board with DecaWave DWM1000 UWB pulse radio module. Each sample includes signal measurements, a real distance, and an environmental label. The signal measurements per sample include a waveform of length 152 and an estimated distance from the device. The environmental label indicates the LOS or NLOS condition. The database consists of two sub databases, generated during two measurement campaigns in different environments. *Database 1-1* was recorded

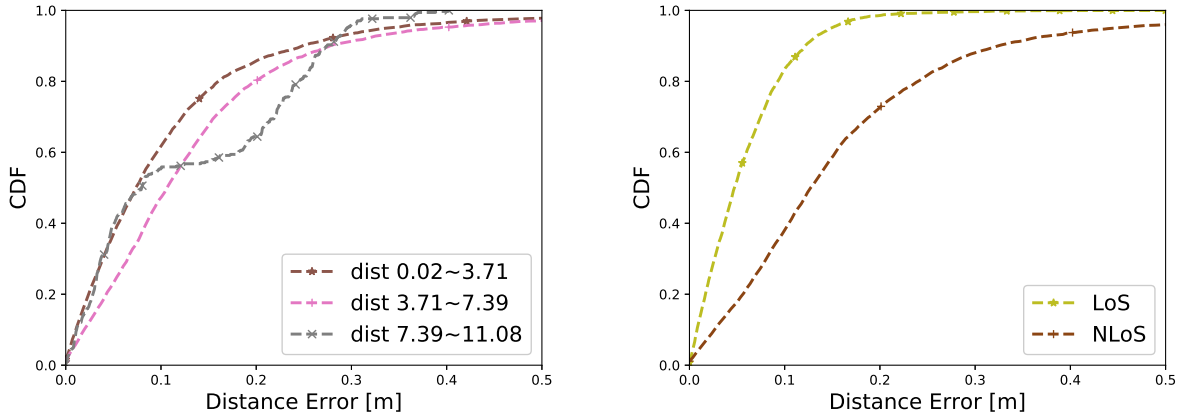

(a) Different Distance Ranges (b) LOS/NLOS conditions

Fig. 6. The CDFs of original measurement errors with respect to distance and environmental scenarios in *Database 2*.

in two adjacent office rooms with a parallel connecting hallway, containing $9,000$ samples in total. *Database 1-2* was recorded in a different office environment involving multiple rooms, containing $25,100$ samples in total.

Database 2: The database is from [48], created using DecaWave EVB1000 devices. Each sample includes signal measurements, a real distance, and an environmental label array. The signal measurements per sample include a waveform of length 157 and an estimated distance from the device. The environmental label array includes two labels for room setting and blocking materials, respectively. The room labels include 5 room scenarios, with i) an outdoor space, ii) a large office room, iii) a medium-size office room, iv) a small office room, and v) a through-the-wall (TTW) environment. The obstacle labels include 10 different materials blocking the LOS path. The database contains $49,233$ data samples in total.

The measurements data are obtained with the two-way ranging (TWR) method equipped to commercial sensing devices, enabled by IEEE 802.15.4-2011 for low-rate network devices [49]. Such ranging method provides cost-effective distance estimates since it does not require synchronization devices. In addition, the proposed model can produce distance estimation with mitigation of different sources of errors including synchronization error, as long as the training measurements and measurements in practical use share similar synchronization error patterns.

We further analyze the dependency of the distance measurement error on different distance ranges and environmental scenarios in *Database 2*, illustrated in Fig. 6. It can be seen that the relationship between distance ranges and measurement errors is more random, while an obvious separation can be viewed between CDFs of LOS and NLOS scenarios. Therefore, the CDFs illustrate that distance measurement error have a strong connection to different environmental scenarios in accordance with the analysis in Section III-A.

B. Datasets

We create four datasets of different measurement settings and environmental resolutions from these databases, presented in Table I. The first two datasets are created from *Database 1* and the last two datasets are from *Database 2*. In particular, *Dataset 2* can be viewed as a generalized version of *Dataset 1*. In *Dataset 2*, training and testing data are generated in different environments by different measurement campaigns to test the generalization of the proposed method. Moreover, *Dataset 4* can be viewed as an elaborated version of *Dataset 3*, with higher resolutions over the obstacle and room labeling. They are targeted to assess the generalization over different environmental scenarios and explore the effect of each environment.

The assignments of environmental labels described above are case studies for environmental identification. Nevertheless, specific labels for environmental identification can be designed with regard to different requirements of practical tasks. For example, different labels such as the LoS, blocked LoS and NLoS conditions of signal measurements can also be explicitly considered by training the proposed model on data with these labels.

C. Network Implementation

The network structure consists of a variational encoder for feature extraction, a corresponding decoder for regularization, an estimator for distance, and an identifier for environmental scenarios. Specifically, the estimator and the identifier are of a simple 4-layer structure, composed of linear layers. The VAE module is designed with a more delicate structure to combine the distance and environmental features generically, as illustrated in Fig. 5b. In particular, the encoder is composed of a parallel structure with similar architectures to disentangle the two features. The architecture for distance feature consists of 3 residual and 4 upsampling blocks, and the one for environmental feature consists of 3 residual blocks and a global pooling layer. Symmetrically, the decoder consists of 3 residual and 4 upsampling blocks for distance features, and a MLP block to produce from environmental feature a

TABLE I
DATASETS FOR CONCURRENT ESTIMATION AND ENVIRONMENTAL IDENTIFICATION

DATASET NAME	DATASET SIZE (TRAIN/TEST)	TRAIN TEST ASSIGNMENTS	ENVIRONMENTAL SCENARIOS LABEL
Dataset 1 (LOS/NLOS)	27790/6998	*Database 1* 80% TRAINING, 20% TESTING RANDOMLY CHOSEN	LOS/NLOS $k \in \mathcal{K}_{\text{LOS}}$
Dataset 2 (ACROSS-ROOM LOS/NLOS)	14798/6451	*Database 1* *Database 1-1* TRAINING *Database 1-2* TESTING	LOS/NLOS $k \in \mathcal{K}_{\text{LOS}}$
Dataset 3 (LOS/NLOS AND OUT/INDOOR)	16999/4250	*Database 2* 80% TRAINING, 20% TESTING RANDOMLY CHOSEN	LOS/NLOS, OUTDOOR/INDOOR $k \in \mathcal{K}_{\text{LOS}} \times \mathcal{K}_{\text{OUTDOOR}}$
Dataset 4 (ROOMS AND OBSTACLES)	16999/4250	*Database 2* 80% TRAINING, 20% TESTING RANDOMLY CHOSEN	5 OBSTACLES, 4 ROOMS $k \in \mathcal{K}_{\text{OBS}} \times \mathcal{K}_{\text{ROOM}}$

TABLE II
FLOPS AND TOTAL PARAMETER NUMBERS OF DL APPROACHES.[1]

EVALUATION METRICS	DISTANCE ESTIMATION CNN	RESNET	LSTM	IINS-VAE
FLOPs	95.51M	108.13M	103.69M	101.26M
PARAM	94.66M	94.66M	94.64M	94.92M

EVALUATION METRICS	ENVIRONMENTAL IDENTIFICATION CNN	RESNET	LSTM	IINS-VAE
FLOPs	95.51M	104.34M	101.21M	96.90M
PARAM	94.67M	94.67M	94.64M	94.66M

set of AdaIN [41] parameters for the residual blocks. The downsampling blocks reduce the dimensionality of signal instances to features while the upsampling blocks generate from features the reconstructed signals. The residual blocks, applied in the bottleneck of the VAE, conduct signal processing without dimensionality changes. The detailed architectures are presented in *Appendix B*.

We use the Adam [50] optimizer with 500 epochs, and the learning rate set to 0.0001. The decays of first and second momentum of gradients are 0.5 and 0.999, respectively. The model is built in Pytorch [51] and conduct learning on a GTX 1080 GPU with a memory of 12 GB with the accelerator powered by the NVIDA Pascal architecture. The code is available to public at https://github.com/JadeLilyx/IIns-VAE.

D. Baseline Methods

We consider three conventional ML-based approaches and three DL approaches as baselines. The ML-based approaches include SVM, Multi-Layer Perceptron (MLP), and Random Forest (RF), while the DL approaches include convolutional neural network (CNN), ResNet, and LSTM. Since these approaches cannot conduct the distance estimation and environmental identification together, we train two separate models for each method, one for distance estimation and one for environmental identification.

The ML-based approaches take physical features (PFs) as inputs to generate the estimations of distance and environmental labels, while DL approaches take in raw measurement data as inputs. In particular, the ML-based approaches can hardly deal with high-dimensional signal measurements. Therefore, we first extract physical features (PFs) as suggested in [9] from the signal measurements. These hand-crafted features account for the intrinsic properties of the wireless link such as its strength, delay, and waveform shape. In addition to RSS and TOA, other PFs are considered such as the maximum amplitude (MA) ν_{MA}, rise time (RT) ν_{RT}, mean excess delay (MED) ν_{MED}, delay spread (DS) ν_{DS}, and kurtosis ν_{kurtosis}. The PFs have been used to obtain DEs and to mitigate the effects of complex propagation of distance-related measurements in the literature [9], [25], [46].

The DL approaches, as the proposed IIns-VAE, take in high-dimensional signals and measured distance directly as inputs. We utilize the same initialization and output layers as IIns-VAE, with their main bodies substituted to CNN, residual, and LSTM blocks of the same depth for a fair comparison. As a main concern for DL approaches, we further compare their computation cost and complexity via FLOPs and parameter numbers in Table II. The results show that the DL approaches have similar computation cost and complexity. In practical usage, the model can be further enhanced with network compression techniques, such as pruning and quantization [52].

The performance comparison on distance estimation is shown in Sec. VI-E, and the comparison on environmental identification is shown in Sec. VI-F. The execution times provided in the manuscript are all conducted on the same GPU device. Note that the proposed approach conducts distance estimation and environmental identification concurrently without the requirement of training separate models as ML and other DL approaches. Therefore, the execution time of the proposed approach in both inference tasks is the same. We also give visualizations of the extracted environmental features

[1]Note that the presented FLOPs values are in terms of MACs (Multiply–Accumulate Operations).

TABLE III
QUANTITATIVE RESULTS ON DISTANCE ESTIMATION ON FOUR DATASETS.

DATA	EVALUATION METRICS	APPROACHES SVM	MLP	RF	CNN	RESNET	LSTM	IINS-VAE
Dataset 1	RMSE	0.218	0.207	0.225	0.420	0.420	0.421	**0.054**
	MAE	0.141	0.138	0.151	0.289	0.289	0.289	**0.028**
	TIME	0.097	0.031	0.031	0.001	0.004	0.408	0.004
Dataset 2	RMSE	0.386	0.558	0.291	0.337	0.339	0.337	**0.275**
	MAE	0.294	0.384	0.226	0.240	0.241	0.241	**0.218**
	TIME	0.064	0.040	0.040	0.001	0.004	0.206	0.004
Dataset 3	RMSE	0.125	0.151	0.132	0.177	0.176	0.177	**0.084**
	MAE	0.082	0.087	0.088	0.124	0.124	0.124	**0.056**
	TIME	0.123	0.040	0.031	0.001	0.005	0.285	0.006
Dataset 4	RMSE	0.162	0.162	0.180	0.218	0.218	0.218	**0.128**
	MAE	0.094	0.096	0.107	0.134	0.134	0.078	**0.069**
	TIME	0.093	0.070	0.071	0.001	0.008	0.386	0.008

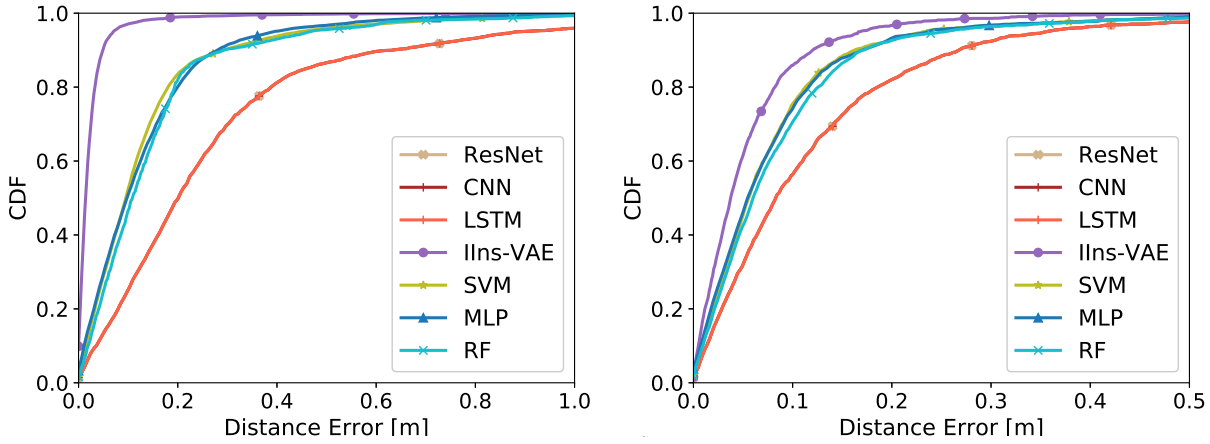

(a) *Dataset 1* (b) *Dataset 3*

Fig. 7. The CDFs of the distance estimation errors for the approaches in comparison.

with reduced dimensionality, presented in Sec. VI-G.

E. Results on Distance Estimation

We evaluate the distance estimation performance of the proposed approach and 6 baseline approaches. The results are presented in Table III. It can be seen that the proposed IIns-VAE achieves the best estimation accuracy and efficiency in all four datasets. Specifically, IIns-VAE can realize a centimeter-level accuracy. The improvements in accuracy to baseline approaches are above 50% for RMSE and above 60% for MAE. In addition, the execution time of IIns-VAE is around 50% shorter than conventional ML-based approaches. The steady performance rise across four datasets illustrates the generalization ability of IIns-VAE in different environmental scenarios. For data from *Database 1*, IIns-VAE and compared approaches achieve better performance on *Dataset 1* for within data campaign training than on *Dataset 2* for cross data campaign training. This indicates that the unseen environmental scenarios remains challenging to predict for the approaches. Moreover, the approaches achieve better performance on *Dataset 3* than on *Dataset 4* for data from *Database 1*. This implies that the complicated environmental features have an essential impact on distance estimation. However, there is almost always an improvement in distance estimation for different environments. This implies that the proposed approach is able to learn a way to disentangle the environmental features and compensate distance error accordingly.

F. Results on Environmental Identification

We evaluate the environmental identification performance of the proposed approach and baseline approaches. The trained proposed IIns-VAE is the same as for distance estimation, while the compared approaches are trained separately for the new identification problem. The results are presented in Table IV. It can be seen that the proposed IIns-VAE shows better performance on *Dataset 1*, *Dataset 3* and *Dataset 4*. Specifically, IIns-VAE achieves the best accuracy in LOS/NLOS identification in *Dataset 1* and indoor/outdoor identification in

TABLE IV
QUANTITATIVE RESULTS ON ENVIRONMENTAL IDENTIFICATION ON FOUR DATASETS.

DATA	EVALUATION METRICS	APPROACHES SVM	MLP	RF	CNN	RESNET	LSTM	IINS-VAE
Dataset 1 (LOS/NLOS)	ACCURACY	0.872	0.899	0.853	0.999	0.999	0.777	**1.000**
	TIME	0.078	0.033	0.033	0.001	0.003	0.290	0.004
Dataset 2 (LOS/NLOS)	ACCURACY	0.771	0.779	0.588	0.668	0.662	**0.804**	0.797
	TIME	0.051	0.044	0.043	0.001	0.003	0.185	0.004
Dataset 3 (LOS/NLOS)	ACCURACY	0.708	0.736	0.696	0.591	0.906	0.524	**0.926**
	TIME	0.0.061	0.032	0.033	0.001	0.004	0.192	0.006
Dataset 3 (IN/OUTDOOR)	ACCURACY	0.962	0.966	0.954	0.908	0.530	0.999	**1.000**
	TIME	0.035	0.031	0.031	0.001	0.004	0.197	0.006
Dataset 4 (5 OBSTACLES)	ACCURACY	0.513	0.531	0.439	0.195	0.195	0.677	**0.713**
	TIME	0.101	0.032	0.033	0.001	0.006	0.223	0.008
Dataset 4 (4 ROOMS)	ACCURACY	0.595	0.376	0.464	0.879	0.846	0.200	**0.880**
	TIME	0.101	0.032	0.032	0.001	0.006	0.228	0.009

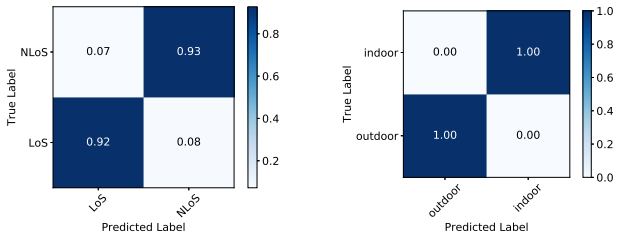

(a) LOS/NLOS Identification. (b) Indoor/Outdoor Identification.

Fig. 8. Confusion matrices for binary identification on *Dataset 3*.

Dataset 3. For *Dataset 2*, IIns-VAE achieves the second best accuracy just after LSTM by 0.007. However, the execution time of IIns-VAE is 96.88% shorter than LSTM. Across different datasest, IIns-VAE also achieves more steady performance than LSTM. The execution time of IIns-VAE is around 50% shorter than ML-based approaches. The efficiency is even more outstanding considering the fact that the presented execution times for IIns-VAE is for concurrent distance estimation and environmental identification instead of a single task.

We further obtain confusion matrices, shown in Fig. 8-9. In particular, the proposed approach achieves over 90% accuracy in LOS/NLOS identification, with the false-alarm rate (0.08) slightly higher than the detection rate (0.07). The approach also achieves high accuracy for multi-class cases. In particular, the approach achieves best performances for metal and wood identification in obstacle identification, and for the 'outdoor' scenario in room identification. Therefore, the proposed approach can conduct highly-accurate identification in all cases analyzed.

G. Environmental Features Visualization

In order to get further insights of environmental semantics, we conduct visualization on latent space. The environmental features $\boldsymbol{z}_e$ from IIns-VAE of testing signal instances are reduced to the 2-dimensionality plane by t-distributed stochastic neighbor embedding (t-SNE) [53]. Each point represents the reduced code of a signal instance, with the color indicating the corresponding environmental scenario. The scatter plots

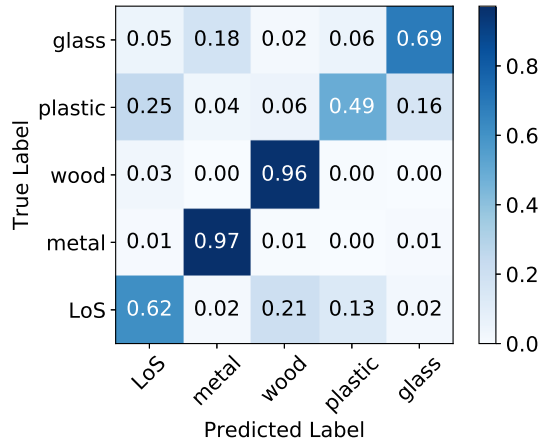

(a) Obstacle Identification.

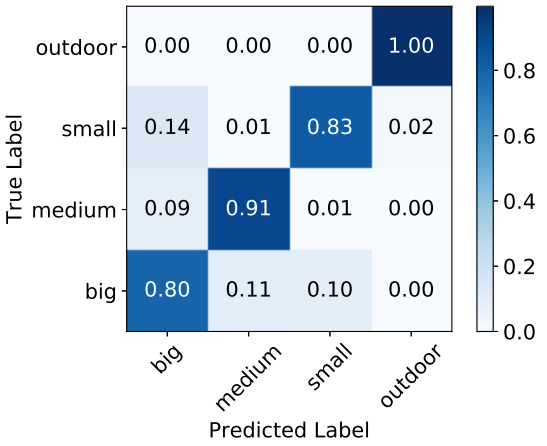

(b) Room Identification.

Fig. 9. Confusion matrices for multi-class identification on *Dataset 4*.

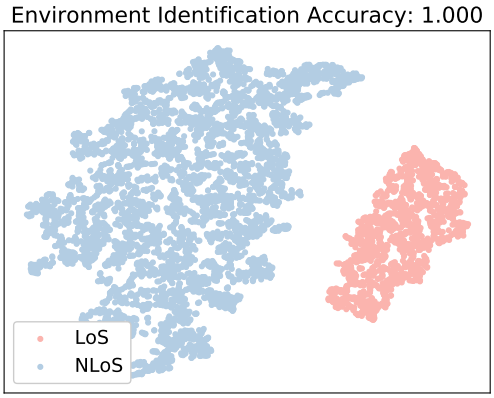

(a) LOS/NLOS features from *Dataset 1*.

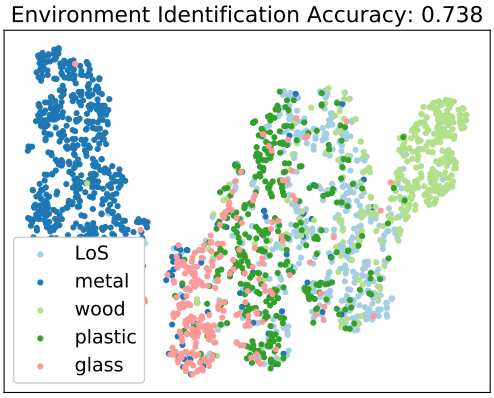

(b) Obstacle features from *Dataset 4*.

Fig. 10. Visualization of environmental features in different obstacle-related scenarios.

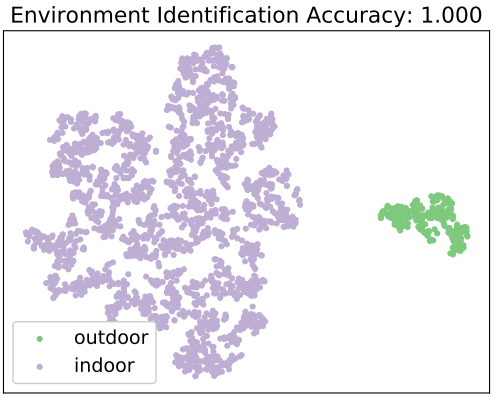

(a) Indoor/Outdoor features from *Dataset 3*.

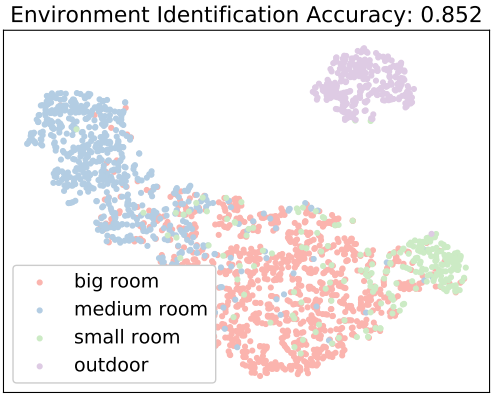

(b) Room features from *Dataset 4*.

Fig. 11. Visualization of environmental features in different room-related scenarios.

are shown in Figs. 10-11.

It can be seen in Fig. 10 that there is a prominent separation for LOS and NLOS conditions, while separations for detailed obstacles are highly related to insulators and conductors. In particular, there is a distinct separation for signal instances from LOS and NLOS conditions in Fig. 10(a). In Fig. 10(b), it can be seen that the metal obstacles are well separated from the others, while the rest three materials are clustered. This implies that insulators and conductors have different effects on received signals. Moreover, a spectrum can be observed among points associated to signals blocked with insulators, along with 'glass-plastic-wood' according to their distance towards 'metal'. This hints at a connection between these obstacles, as they possess the same order of dielectric coefficient values. Slight overlapping among different classes also indicates that the impact of obstacle-related environmental features is challenging to fully disentangle and exploit. Nevertheless, this reveals a possible structure of the underlying manifold to conduct propagation identification with respect to NLOS conditions and detailed obstacle labels.

Similar visualizations are conducted for room-related environmental scenarios, shown in Fig. 11. It can be seen in Fig. 11(a) that there is a distinct separation for indoor and outdoor scenarios. This explains the drastic difference between indoor and outdoor environments, and why existing methods find it challenging to generalize in both indoor and outdoor conditions. Visualization on different room scenarios are shown in Fig. 11(b). It can be seen that points of different room labels gather in slightly-overlapping clusters, while the outdoor points are in clear separation. This reveals a possible structure for environmental identification with respect to different room scenarios. Moreover, clusters of different room scenarios relatively have less overlaps than those of obstacle scenarios. According to the analysis in section III-A, obstacle-related features mostly impact FPs of received signals, while room-related features impact both FPs and MPCs. This implies that room-related features and their impact on received signals are more exploitable than obstacle-related ones, in accordance with the quantitative results in sections VI-E and VI-F.

VII. Conclusion

This paper proposed a DL-based approach named IIns-VAE to conduct concurrent inference on distance and environmental scenarios for wireless applications. The proposed approach

enabled highly efficient distance estimation and environmental identification, and extracted distance and environmental features automatically from received signals. Specifically, the approach presented an LVM for the propagated signal measurements, consisting of a distance-related latent variable and an environment-related variable. Then a VAE-based network was introduced to approximate the inference on such LVM via deep learning and a loss function is derived from the variational bound. The proposed approach integrated benefits from both statistical and deep learning techniques. Experimental results illustrated the superiority on distance estimation and environmental identification compared to conventional approaches. Future work will focus on the scalability of the approach towards more complicated problems, aiming to enable easy and enhanced situational awareness in the next generation of wireless applications.

APPENDIX A
PROOF OF *Proposition 1*

We denote latent variable $\boldsymbol{z} = \{\boldsymbol{z}_\mathrm{d}, \boldsymbol{z}_\mathrm{e}\}$ and label variable $\boldsymbol{y} = \{d, k\}$ for convenience. The bound can be derived as

$$\begin{aligned}
&\log p(\boldsymbol{x}, \boldsymbol{y}) \\
&\geq \log p(\boldsymbol{x}, \boldsymbol{y}) - \mathrm{D}_{\mathrm{KL}}\left(q(\boldsymbol{z}|\boldsymbol{x}, \boldsymbol{y})\middle\|p(\boldsymbol{z}|\boldsymbol{x}, \boldsymbol{y})\right) \\
&= \int q(\boldsymbol{z}|\boldsymbol{x}, \boldsymbol{y}) \log \frac{p(\boldsymbol{x}, \boldsymbol{y})p(\boldsymbol{z}|\boldsymbol{x}, \boldsymbol{y})}{q(\boldsymbol{z}|\boldsymbol{x}, \boldsymbol{y})} d\boldsymbol{z} \\
&= \int q(\boldsymbol{z}|\boldsymbol{x}, \boldsymbol{y}) \log p(\boldsymbol{x}, \boldsymbol{y}|\boldsymbol{z}) d\boldsymbol{z} \\
&\quad - \int q(\boldsymbol{z}|\boldsymbol{x}, \boldsymbol{y}) \log \frac{q(\boldsymbol{z}|\boldsymbol{x}, \boldsymbol{y})}{p(\boldsymbol{z})} d\boldsymbol{z} \\
&= \mathbb{E}_{q(\boldsymbol{z}|\boldsymbol{x}, \boldsymbol{y})}\left\{\log p(\boldsymbol{x}, \boldsymbol{y}|\boldsymbol{z})\right\} - \mathrm{D}_{\mathrm{KL}}\left(q(\boldsymbol{z}|\boldsymbol{x}, \boldsymbol{y})\middle\|p(\boldsymbol{z})\right) \\
&= \mathbb{E}_{q(\boldsymbol{z}|\boldsymbol{x})}\left\{\log p(\boldsymbol{x}|\boldsymbol{z})p(\boldsymbol{y}|\boldsymbol{z})\right\} - \mathrm{D}_{\mathrm{KL}}\left(q(\boldsymbol{z}|\boldsymbol{x})\middle\|p(\boldsymbol{z})\right) \\
&= \mathbb{E}_{q(\boldsymbol{z}|\boldsymbol{x})}\left\{\log p(\boldsymbol{x}|\boldsymbol{z})\right\} + \mathbb{E}_{q(\boldsymbol{z}|\boldsymbol{x})}\left\{\log p(\boldsymbol{y}|\boldsymbol{z})\right\} \\
&\quad - \mathrm{D}_{\mathrm{KL}}\left(q(\boldsymbol{z}|\boldsymbol{x})\middle\|p(\boldsymbol{z})\right) \\
&= \mathbb{E}_{q(\boldsymbol{z}_\mathrm{d}, \boldsymbol{z}_\mathrm{e}|\boldsymbol{x}; \boldsymbol{\phi})}\left\{\log p(\boldsymbol{x}|\boldsymbol{z}_\mathrm{d}, \boldsymbol{z}_\mathrm{e}; \boldsymbol{\theta})\right\} \\
&\quad + \mathbb{E}_{q(\boldsymbol{z}_\mathrm{d}|\boldsymbol{x}; \boldsymbol{\phi})}\left\{\log p(d|\boldsymbol{z}_\mathrm{d}; \boldsymbol{\varphi})\right\} \\
&\quad + \mathbb{E}_{q(\boldsymbol{z}_\mathrm{e}|\boldsymbol{x}; \boldsymbol{\phi})}\left\{\log p(k|\boldsymbol{z}_\mathrm{e}; \boldsymbol{\varphi})\right\} \\
&\quad - \mathrm{D}_{\mathrm{KL}}\left(q(\boldsymbol{z}_\mathrm{d}, \boldsymbol{z}_\mathrm{e}|\boldsymbol{x}; \boldsymbol{\phi})\middle\|p(\boldsymbol{z}_\mathrm{d}, \boldsymbol{z}_\mathrm{e})\right) \\
&=: \mathcal{L}_{\mathrm{ELBO}}(\boldsymbol{x}, d, k; \boldsymbol{\phi}, \boldsymbol{\theta}, \boldsymbol{\varphi})
\end{aligned} \tag{23}$$

Note that the third to last equation in (23) are derived according to the LVM assumptions in (9), using

$$\begin{aligned}
&q(\boldsymbol{z}|\boldsymbol{x}, \boldsymbol{y}) = q(\boldsymbol{z}|\boldsymbol{x}),\ q(\boldsymbol{z}|\boldsymbol{x}, \boldsymbol{y}) = q(\boldsymbol{z}|\boldsymbol{x}) \\
&p(\boldsymbol{x}, \boldsymbol{y}|\boldsymbol{z}) = p(\boldsymbol{x}|\boldsymbol{y}, \boldsymbol{z})p(\boldsymbol{y}|\boldsymbol{z}) = p(\boldsymbol{x}|\boldsymbol{z})p(\boldsymbol{y}|\boldsymbol{z}).
\end{aligned}$$

The last equation in (23) is derived from the LVM assumptions in (6)-(8) as well as the notation exchange for $\boldsymbol{y}$ and $\boldsymbol{z}$, i.e.,

$$p(\boldsymbol{y}|\boldsymbol{z}) = \ p(d, k|\boldsymbol{z}_\mathrm{d}, \boldsymbol{z}_\mathrm{e}) = \ p(d|\boldsymbol{z}_\mathrm{d})p(k|\boldsymbol{z}_\mathrm{e}).$$

APPENDIX B
DETAILED NETWORK ARCHITECTURE

The detailed network architecture for the proposed IIns-VAE are presented in Table V-VI, including the layer type, output shape, and trainable parameters. Note that '-1' in the first dimension of output shape is adaptive to the batch size of data instances. The output shape of the identifier in Table VI, currently 2, can be adaptive to the class number of environmental scenarios, e.g., 5 for identification of obstacles and 4 for rooms.

REFERENCES

[1] H. Uzunboylu, N. Cavus, and E. Ercag, "Using mobile learning to increase environmental awareness," *Comput. & Educ.*, vol. 52, no. 2, pp. 381–389, Nov. 2008.

[2] H. Celebi, I. Guevenc, S. Gezici, and H. Arslan, "Cognitive-radio systems for spectrum, location, and environmental awareness," *IEEE Antennas and Propag. Mag.*, vol. 52, no. 4, pp. 41–61, Nov. 2010.

[3] R. Mendrzik, F. Meyer, G. Bauch, and M. Win, "Enabling situational awareness in millimeter wave massive MIMO systems," *IEEE J. Sel. Topics Signal Process.*, vol. 13, no. 5, pp. 1196–1211, Aug. 2019.

[4] M. Page and T. L. Wickramarathne, "Enhanced situational awareness with signals of opportunity: RSS-based localization and tracking," in *Proc. IEEE Int. Conf. Intell. Transport. Syst.*, Oct. 2019, pp. 3833–3838.

[5] M. Z. Win, Y. Shen, and W. Dai, "A theoretical foundation of network localization and navigation," *Proc. IEEE*, vol. 106, no. 7, pp. 1136–1165, Jul. 2018.

[6] M. Z. Win, W. Dai, Y. Shen, G. Chrisikos, and H. Vincent Poor, "Network operation strategies for efficient localization and navigation," *Proc. IEEE*, vol. 106, no. 7, pp. 1224–1254, Jul. 2018.

[7] Y. Shen, H. Wymeersch, and M. Z. Win, "Fundamental limits of wideband localization – Part II: Cooperative networks," *IEEE Trans. Inf. Theory*, vol. 56, no. 10, pp. 4981–5000, Oct. 2010.

[8] K. Rickard and G. Fredrik, "The future of automotive localization algorithms: Available, reliable, and scalable localization: Anywhere and anytime," *IEEE Signal Process. Mag.*, vol. 34, no. 2, pp. 60–69, Mar. 2017.

[9] H. Wymeersch, S. Maranò, W. M. Gifford, and M. Z. Win, "A machine learning approach to ranging error mitigation for UWB localization," *IEEE Trans. Commun.*, vol. 60, pp. 1719–1728, Apr. 2012.

[10] Z. Xiao, H. Wen, A. Markham, A. Trigoni, P. Blunsom, and J. Frolik, "Non-line-of-sight identification and mitigation using received signal strength," *IEEE Trans. Commun.*, vol. 14, no. 3, pp. 1689–1702, Mar. 2015.

[11] T. Nguyen, Y. Jeong, H. Shin, and M. Win, "Machine learning for wideband localization," *IEEE J. Sel. Areas Commun.*, vol. 33, no. 7, pp. 1357–1380, Jul. 2015.

[12] A. Decurninge, L. G. Ordóñez, P. Ferrand, G. He, B. Li, W. Zhang, and M. Guillaud, "CSI-based outdoor localization for massive MIMO: Experiments with a learning approach," in *Proc. Int. Symp. on Wireless Commun. Sys.*, Aug. 2018, pp. 1–6.

[13] Z. Flavio and C. Andrea, "Inhomogeneous poisson sampling of finite-energy signals with uncertainties in $\mathbb{R}^d$," *IEEE Trans. Signal Process.*, vol. 64, no. 18, pp. 4679–4694, Apr. 2016.

[14] D. Dardari, A. Conti, C. Buratti, and R. Verdone, "Mathematical evaluation of environmental monitoring estimation error through energy-efficient wireless sensor networks," *IEEE Trans. Mob. Comput.*, vol. 6, no. 7, pp. 790–802, May 2007.

[15] C. Giuseppe, F. Luca, B. Paolo, C. Antonio, B. Cristian, T. Manoop, and C. Reza, "Fostering participaction in smart cities: a geo-social crowdsensing platform," *IEEE Commun Mag.*, vol. 51, no. 6, pp. 112–119, Jun. 2013.

[16] Z. Yu, Z. Liu, F. Meyer, A. Conti, and M. Win, "Localization based on channel impulse response estimates," in *Proc. IEEE Position Location and Navig. Symp. (PLANS)*, Jun. 2020, pp. 1014–1021.

[17] M. Kotaru, K. Joshi, D. Bharadia, and S. Katti, "SpotFi: Decimeter level localization using WiFi," in *Proc. ACM Special Interest Group on Data Commun. (ACM SIGCOMM)*, Aug. 2015, pp. 269–282.

[18] K. Johan, W. Shurjeel, A. Peter, T. Fredrik, and M. A. F., "A measurement-based statistical model for industrial ultra-wideband channels," *IEEE Trans. Wireless Commun.*, vol. 6, no. 8, pp. 3028–3037, Aug. 2007.

[19] M. Z. Win, G. Chrisikos, and A. F. Molisch, "Wideband diversity in multipath channels with nonuniform power dispersion profiles," *IEEE Trans. Wireless Commun.*, vol. 5, no. 5, pp. 1014–1022, Jun. 2006.

[20] U. A. Khan, S. Kar, and J. M. F. Moura, "Diland: An algorithm for distributed sensor localization with noisy distance measurements," *IEEE Trans. Signal Process.*, vol. 58, no. 3, pp. 1940–1947, Mar. 2010.

TABLE V
ARCHITECTURE OF VAIRATIONAL ENCODER FOR DISTANCE AND ENVIRONMENTAL FEATURES EXTRACTION

VARIATIONAL ENCODER (DISTANCE/ENVIRONMENTAL FEATURES PATHS)					
LAYER TYPE	OUTPUT SHAPE	PARAM	LAYER TYPE	OUTPUT SHAPE	PARAM
LINEAR-RELU	$[-1, 4096]$	94.6M	LINEAR-RELU	$[-1, 4096]$	94.6M
CONV2D-IN2D-RELU	$[-1, 4, 64, 64]$	200	CONV2D-RELU	$[-1, 4, 64, 64]$	200
CONV2D-IN2D-RELU	$[-1, 8, 32, 32]$	520	CONV2D-RELU	$[-1, 8, 32, 32]$	520
CONV2D-IN2D-RELU	$[-1, 16, 16, 16]$	2,064	CONV2D-RELU	$[-1, 16, 16, 16]$	2,064
CONV2D-IN2D-RELU	$[-1, 32, 8, 8]$	8,224	CONV2D-RELU	$[-1, 16, 8, 8]$	4,112
CONV2D-IN2D-RELU	$[-1, 64, 4, 4]$	32,832	CONV2D-RELU	$[-1, 16, 4, 4]$	4,112
RESBLOCK2D	$[-1, 64, 4, 64]$	73,856	CONV2D-RELU	$[-1, 16, 2, 2]$	4,112
RESBLOCK2D	$[-1, 64, 4, 64]$	73,856	CONV2D-RELU	$[-1, 16, 1, 1]$	4,112
RESBLOCK2D	$[-1, 64, 4, 64]$	73,856	AVGPOOL2D	$[-1, 16, 1, 1]$	0
LINEAR-RELU	$[-1, 16]$	16,400	CONV2D	$[-1, 16, 1, 1]$	272

TABLE VI
ARCHITECTURE OF DISTANCE ESTIMATOR AND ENVIRONMENTAL IDENTIFIER

DISTANCE ESTIMATOR / ENVIRONMENTAL IDENTIFIER		
LAYER TYPE	OUTPUT SHAPE	PARAM
LINEAR-LEAKYRELU	$[-1, 256]$ / $[-1, 16]$	4,352 / 272
LINEAR-LEAKYRELU	$[-1, 128]$ / $[-1, 32]$	32,896 / 544
LINEAR-LEAKYRELU	$[-1, 16]$ / $[-1, 2]$	2,064 / 66

[21] A. H. Sayed, A. Tarighat, and N. Khajehnouri, "Network-based wireless location: challenges faced in developing techniques for accurate wireless location information," *IEEE Signal Process. Mag.*, vol. 22, no. 4, pp. 24–40, Jun. 2005.

[22] S. Venkatraman, J. Caffery, and H.-R. You, "Location using LOS range estimation in NLOS environments," in *Proc. IEEE Semiannual Veh. Technol. Conf.*, vol. 2, May 2002, pp. 856–860 vol.2.

[23] S. Maranò, W. M. Gifford, H. Wymeersch, and M. Z. Win, "NLOS identification and mitigation for localization based on UWB experimental data," *IEEE J. Sel. Areas Commun.*, vol. 28, no. 7, pp. 1026–1035, Sep. 2010.

[24] Z. Xiao, H. Wen, A. Markham, A. Trigoni, P. Blunsom, and J. Frolik, "Identification and mitigation of non-line-of-sight conditions using received signal strength," in *IEEE Int. Conf. on Wireless and Mobile Comput., Netw. and Commun. (WiMob)*, 2013, pp. 667–674.

[25] S. Mazuelas, A. Conti, J. C. Allen, and M. Z. Win, "Soft range information for network localization," *IEEE Trans. Signal Process.*, vol. 66, no. 12, pp. 3155–3168, Jun. 2018.

[26] A. Conti, S. Mazuelas, S. Bartoletti, W. Lindsey, and M. Win, "Soft information for localization-of-things," *Proc. IEEE*, vol. 107, pp. 2240–2264, Sep. 2019.

[27] C. Mao, K. Lin, T. Yu, and Y. Shen, "A probabilistic learning approach to UWB ranging error mitigation," *Proc. IEEE Global Telecomm. Conf.*, pp. 1–6, 2018.

[28] S. Angarano, V. Mazzia, F. Salvetti, G. Fantin, and M. Chiaberge, "Robust ultra-wideband range error mitigation with deep learning at the edge," *ArXiv*, vol. abs/2011.14684, May 2020.

[29] S. Haoran, K. A. Ozge, M. Mike, V. Harish, and H. Mingyi, "Deep learning based preamble detection and TOA estimation," in *Proc. IEEE Global Telecomm. Conf.*, Dec. 2019, pp. 1–6.

[30] Y. Li, S. Mazuelas, and Y. Shen, "Deep generative model for simultaneous range error mitigation and environment identification," in *Proc. IEEE Global Telecomm. Conf.*, Dec. 2021, pp. 1–6.

[31] ——, "A deep learning approach for generating soft range information from RF data," in *Proc. IEEE Global Telecomm. Conf. Workshop (GC Wkshps)*, Dec. 2021.

[32] D. Burghal, A. T. Ravi, V. Rao, A. A. Alghafis, and A. F. Molisch, "A comprehensive survey of machine learning based localization with wireless signals," *arXiv preprint arXiv:2012.11171*, Dec. 2020.

[33] P. Meissner and K. Witrisal, "Multipath-assisted single-anchor indoor localization in an office environment," in *Proc. Int. Conf. Systems, Signals Image Process.*, Vienna, Austria, Apr. 2012, pp. 22–25.

[34] K. S. Kim, "Hybrid building/floor classification and location coordinates regression using a single-input and multi-output deep neural network for large-scale indoor localization based on wi-fi fingerprinting," in *2018 Sixth International Symposium on Computing and Networking Workshops (CANDARW)*. IEEE, Nov. 2018, pp. 196–201.

[35] K. Witrisal, P. Meissner, E. Leitinger, Y. Shen, C. Gustafson, F. Tufvesson, K. Haneda, D. Dardari, A. F. Molisch, A. Conti, and M. Z. Win, "High-accuracy localization for assisted living: 5G systems will turn multipath channels from foe to friend," *IEEE Signal Processing Magazine*, vol. 33, no. 2, pp. 59–70, Mar. 2016.

[36] J. Kulmer, S. Hinteregger, B. Grobwindhager, M. Rath, M. S. Bakr, E. Leitinger, and K. Witrisal, "Using decawave UWB transceivers for high-accuracy multipath-assisted indoor positioning," in *Proc. IEEE Int. Conf. Commun. Workshop*, Jul. 2017, pp. 1239–1245.

[37] A. F. Molisch, "Wireless communications," *John Wiley & Sons*, 2012.

[38] D. M. Blei, A. Kucukelbir, and J. D. McAuliffe, "Variational inference: A review for statisticians," *J. Am. Statist. Assoc.*, vol. 112, no. 518, pp. 859–877, 2017.

[39] D. Ulyanov, A. Vedaldi, and V. Lempitsky, "Instance normalization: The missing ingredient for fast stylization," *arXiv preprint arXiv:1607.08022*, 2016.

[40] D. P. Kingma and M. Welling, "Auto-encoding variational bayes," *arXiv preprint arXiv:1312.6114*, 2013.

[41] X. Huang and S. Belongie, "Arbitrary style transfer in real-time with adaptive instance normalization," in *Proc. IEEE Int. Conf. on Comput. Vision (ICCV)*, Oct. 2017, pp. 1501–1510.

[42] J. Chou, C. Yeh, and H. Lee, "One-shot voice conversion by separating speaker and content representations with instance normalization," *arXiv preprint arXiv:1904.05742*, 2019.

[43] Y. Li, S. Mazuelas, and Y. Shen, "A Semi-Supervised Learning Approach for Ranging Error Mitigation Based on UWB Waveform," in *Proc. Military Commun. Conf.*, Dec. 2021, pp. 533–537.

[44] ——, "Deep GEM-Based Network for Weakly Supervised UWB Ranging Error Mitigation," in *Proc. Military Commun. Conf.*, Dec. 2021, pp. 528–532.

[45] Z. Zhou, "A brief introduction to weakly supervised learning," *Natl. Sci. Res.*, vol. 5, no. 1, pp. 44–53, 2018.

[46] S. Mazuelas and A. Pérez, "General supervision via probabilistic transformations," in *Eur. Conf. on Artif. Intell. (ECAI)*, Aug. 2020, pp. 1348–1354.

[47] K. Bregar and M. Mohori, "Improving indoor localization using convolutional neural networks on computationally restricted devices," *IEEE Access*, vol. 6, pp. 17 429–17 441, 2018.

[48] S. Angarano, F. Salvetti, V. Mazzia, G. Fantin, and M. Chiaberge, "Deep UWB: A dataset for uwb ranging error mitigation in indoor environments." [OL], https://zenodo.org/record/4290069.X75qYc3-3Dc.

[49] "Ieee standard for local and metropolitan area networks – part 15.4: Low-rate wireless personal area networks (lr-wpans)," *IEEE Std 802.15.4-2011*, 2011.

[50] D. P. Kingma and J. L. Ba, "Adam: A method for stochastic optimization," *arXiv preprint arXiv:1412.6980*, 2014.

[51] A. Paszke, S. Gross, S. Chintala, G. Chanan, E. Yang, Z. DeVito, Z. Lin, A. Desmaison, L. Antiga, and A. Lerer, "Automatic differentiation in PyTorch," *Neural Inf. Process. Syst. Workshop (NIPS Wkshps)*, 2017.
[52] A. Alqahtani, X. Xie, and M. W. Jones, "Literature review of deep network compression," *Informatics*, vol. 8, no. 4(77), 2021.
[53] L. Van der Maaten and G. Hinton, "Visualizing data using t-SNE." *J. Mach. Learn. Res.*, vol. 9, no. 11, 2008.

Yuxiao Li (Student Member, IEEE) received the B.E. degree (Hons.) in electronic engineering with a minor in computer science from Xidian University, Xi'an, China, in 2018. She is currently working toward the Ph.D. degree with the Department of Electronic Engineering, Tsinghua University.

Her current research interests include theoretical frameworks to implement deep learning techniques in complicated statistic inference problems and their applications in indoor localization and situational awareness.

Santiago Mazuelas (Senior Member, IEEE) received the Ph.D. in Mathematics and Ph.D. in Telecommunications Engineering from the University of Valladolid, Spain, in 2009 and 2011, respectively.

He is currently Ikerbasque Associate Researcher at the Basque Center for Applied Mathematics (BCAM). Prior to joining BCAM, he was a Staff Engineer at Qualcomm Corporate Research and Development from 2014 to 2017. He previously worked from 2009 to 2014 as Postdoctoral Fellow and Associate in the Wireless Information and Network Sciences Laboratory at the Massachusetts Institute of Technology (MIT). Dr. Mazuelas has been Area Editor for the IEEE COMMUNICATIONS LETTERS from 2017 to 2022, and served as Technical Program Vice-chair at the 2021 IEEE Globecom. His papers have received the IEEE Communications Society Fred W. Ellersick Prize in 2012 the SEIO-FBBVA Best Applied Contribution in the Statistics Field in 2022, and Best Paper Awards from the IEEE ICC, the IEEE ICUWB, and the IEEE Globecom.

Yuan Shen (Senior Member, IEEE) received the B.E. degree in electronic engineering from Tsinghua University in 2005, and the S.M. and Ph.D. degrees in electrical engineering and computer science from the Massachusetts Institute of Technology (MIT) in 2008 and 2014, respectively.

He is currently a Professor with the Department of Electronic Engineering, Tsinghua University. His research interests include network localization and navigation, integrated sensing and control, and multi-agent systems. His papers have received the IEEE ComSoc Fred W. Ellersick Prize and several best paper awards from IEEE conferences. He has served as the TPC Symposium Co-Chair for IEEE ICC and IEEE Globecom for several times. He was the Elected Chair for the IEEE ComSoc Radio Communications Committee from 2019 to 2020. He is an Editor of the IEEE TRANSACTIONS ON COMMUNICATIONS, IEEE TRANSACTIONS ON WIRELESS COMMUNICATIONS, IEEE WIRELESS COMMUNICATIONS LETTERS, and *China Communications*.